

LA-UR-15-27833

Approved for public release; distribution is unlimited.

Title: Accelerator-driven X-ray Sources

Author(s): Nguyen, Dinh Cong

Intended for: 2015 IEEE Nuclear Science Symposium and Medical Imaging Conference,
2015-10-31 (San Diego, California, United States)

Issued: 2015-11-09 (rev.2)

Disclaimer:

Los Alamos National Laboratory, an affirmative action/equal opportunity employer, is operated by the Los Alamos National Security, LLC for the National Nuclear Security Administration of the U.S. Department of Energy under contract DE-AC52-06NA25396. By approving this article, the publisher recognizes that the U.S. Government retains nonexclusive, royalty-free license to publish or reproduce the published form of this contribution, or to allow others to do so, for U.S. Government purposes. Los Alamos National Laboratory requests that the publisher identify this article as work performed under the auspices of the U.S. Department of Energy. Los Alamos National Laboratory strongly supports academic freedom and a researcher's right to publish; as an institution, however, the Laboratory does not endorse the viewpoint of a publication or guarantee its technical correctness.

Accelerator-driven X-ray Sources

Dinh C. Nguyen
Los Alamos National Laboratory

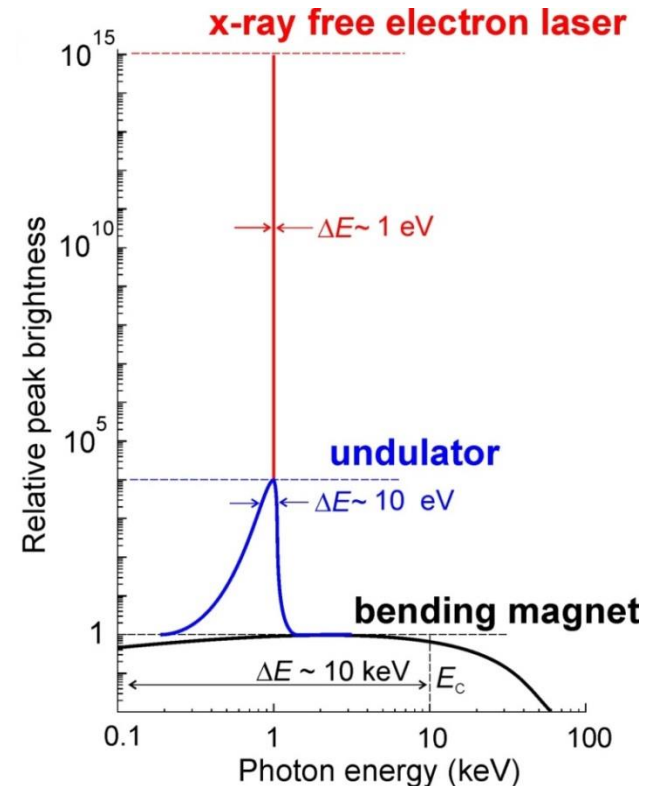
November 1st, 2015

2015 IEEE Nuclear Science Symposium & Medical Imaging Conference
22nd International Symposium on Room-Temperature X-ray and Gamma-ray Detectors

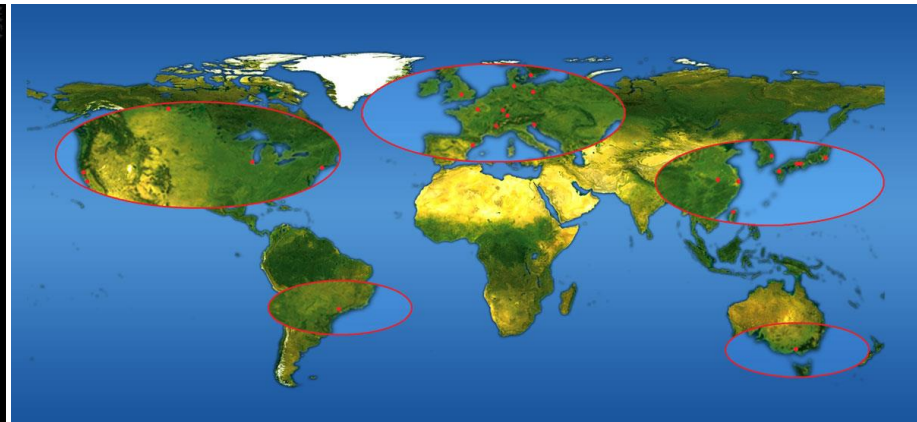
Accelerator-driven Light Sources
Short Course

Course Outline

- Introduction
- Synchrotron Radiation
 - Bending magnet radiation
 - Wiggler radiation
 - Undulator radiation
 - Brightness and brilliance definition
 - Synchrotron radiation facilities
- X-ray Free-Electron Lasers
 - Linac-driven X-ray FEL
 - FEL interactions
 - Self-amplified spontaneous emission (SASE)
 - SASE self-seeding
 - Fourth-generation light source facilities
- Other X-ray Sources
 - Energy Recovery Linac
 - Inverse Compton scattering
 - Laser wakefield accelerator driven X-rays sources



Introduction



Space image shows where visible light is made on Earth.

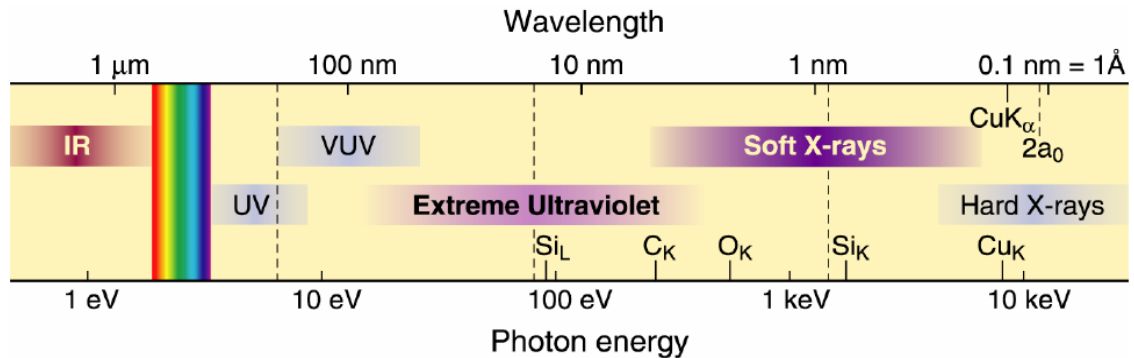
For aliens with X-ray vision, only a few red dots are visible.

X-rays are a form of electromagnetic waves in the 300 eV – 30 keV energy range.

X-ray tubes produce broadband Bremsstrahlung (and a few atomic lines) when electrons are decelerated in a metal target.

Energy-wavelength relation

$$h\nu[eV] = \frac{1,240}{\lambda[nm]}$$



X-ray Source Overview

- **X-ray Tubes**

- X-ray tubes emit **Bremsstrahlung** and **characteristic peaks**
- Bremsstrahlung is broadband, low-brilliance X-rays
- Characteristic peaks are narrow-line atomic transitions

- **Synchrotron Radiation (3rd Generation Light Sources)**

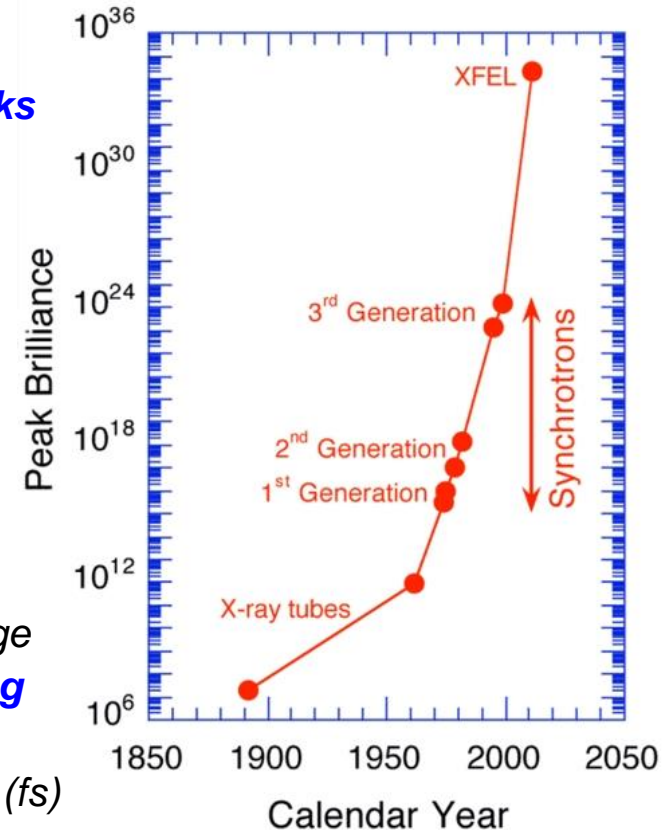
- Electrons in storage rings produce **synchrotron radiation**
- **Bending magnet** and **wiggler radiation** is broadband
- **Undulator radiation** has narrow spectral lines

- **X-ray Free-Electron Lasers (4th Generation Light Sources)**

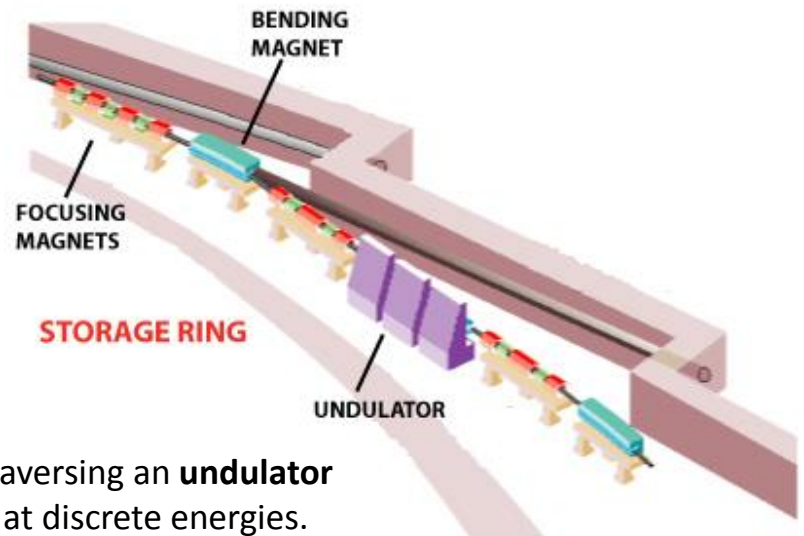
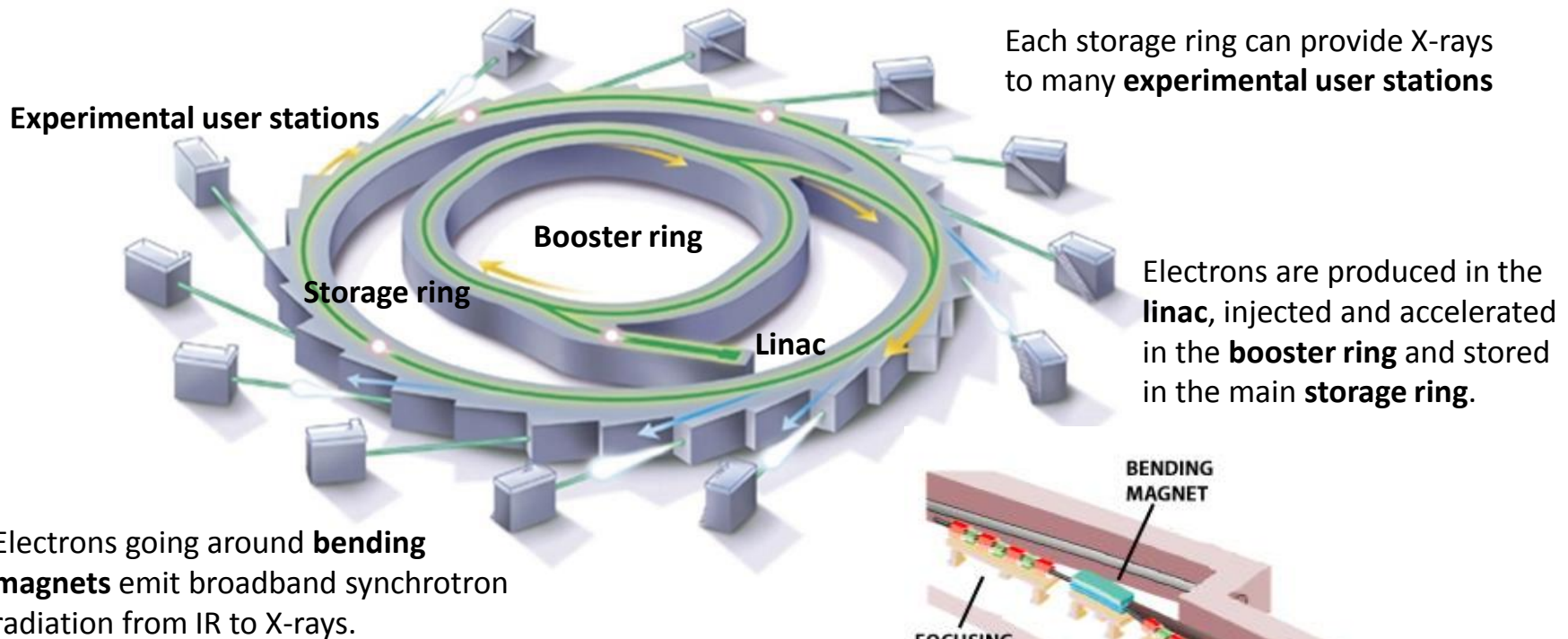
- **Resonance condition** enables continuous energy exchange
- Electrons undergo **energy modulation** and **microbunching**
- Microbunched electrons emit **coherent radiation**
- Linac-driven **XFEL** is tunable, monochromatic and ultrafast (fs)

- **Other Techniques**

- Energy Recovery Linac (**ERL**) produces partially coherent undulator radiation
- **Inverse Compton Scattering** produce incoherent gamma rays
- X-rays can be produced by electrons from **laser-wakefield accelerators**



Storage Rings



Electrons traversing an **undulator** emit X-rays at discrete energies.

Review of Special Relativity

The **relativistic Lorentz factor**, γ is the total electron beam energy (kinetic energy + rest energy) divided by electron rest mass energy ($m_e c^2 = 0.511$ MeV). The more common equation for γ in term of β , the electron's **relative velocity** to the speed of light c , is also given below

$$\gamma = \frac{E_b + m_e c^2}{m_e c^2} \quad \gamma = \frac{1}{\sqrt{1 - \beta^2}} \quad \text{where} \quad \beta = \frac{v}{c}$$

In many light sources, the energy of electron beams used to make X-rays are GeV-ish, much higher than the electron rest mass energy. Thus, γ can be approximated as

$$\gamma \approx \frac{E_b}{m_e c^2} = 1957 E_b [\text{GeV}]$$

It is straightforward to find β from γ by rearranging the expression for γ^2 to obtain $\beta^2 = 1 - \frac{1}{\gamma^2}$ then approximate the square root of $\beta^2 = 1 - \frac{1}{\gamma^2}$ knowing $\frac{1}{\gamma^2} \ll 1$.

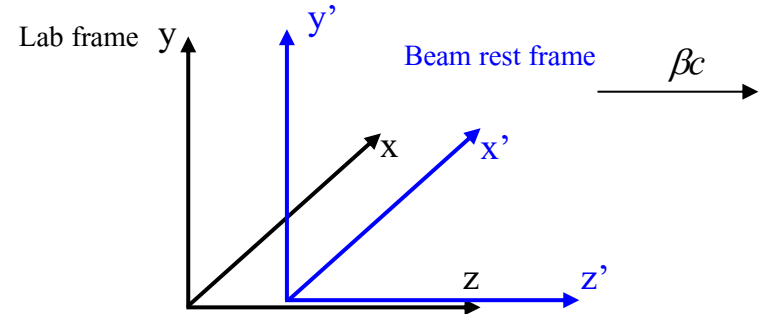
$$\beta \approx 1 - \frac{1}{2\gamma^2}$$

For 1-GeV electron beam, $\gamma \sim 1957$ and $\beta = 0.9999997$

Relativistic Length Contraction

Frame of reference

It is often convenient to change our frame of reference from the Lab frame to the beam rest frame, shown here traveling to the right with respect to the Lab frame at speed $v = \beta c$



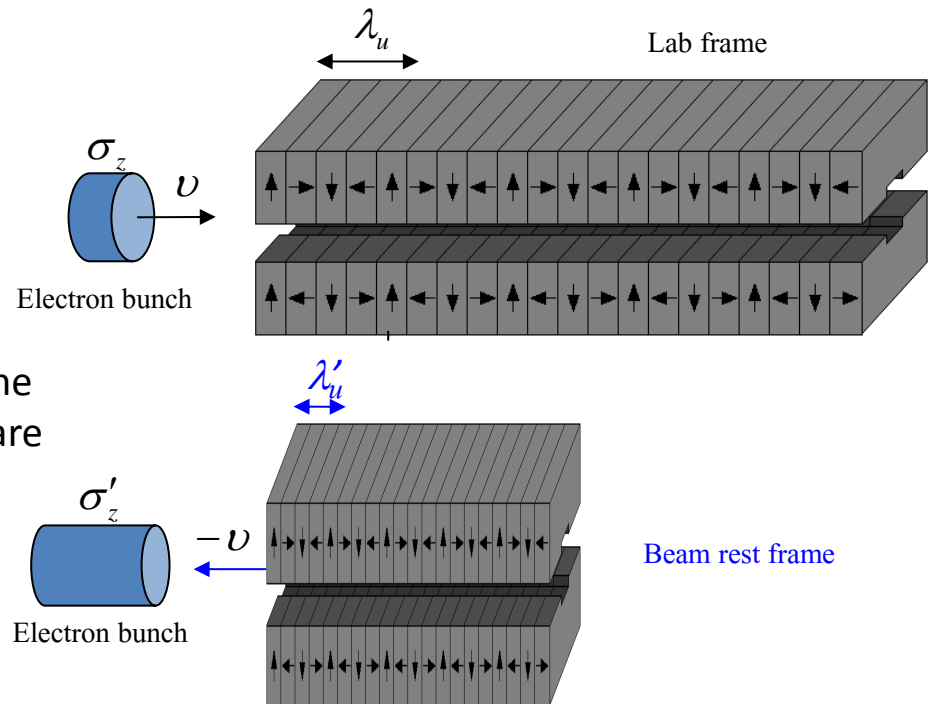
Length contraction

In the Lab frame, the length of an electron bunch appears short and the undulator, being at rest, has the longest length.

$$\sigma_z \approx c \sigma_t$$

In the beam rest frame, the electron bunch is the longest while the undulator period and length are contracted by the Lorentz relativistic factor γ

$$\sigma'_z = \gamma \sigma_z \quad \lambda'_u = \frac{\lambda_u}{\gamma}$$



Relativistic Doppler Shift

Consider a source of radiation with frequency ω_s in its rest frame. The source is moving toward an observer at angle ϕ with respect to the direction of observation. The observed frequency ω_o differs from the source frequency ω_s due to relativistic Doppler effects.

Relativistic Doppler frequency up-shift

$$\omega_o = \frac{\omega_s}{\gamma(1 - \beta \cos \phi)}$$

$\phi = 0^\circ$ (source moving toward observer)

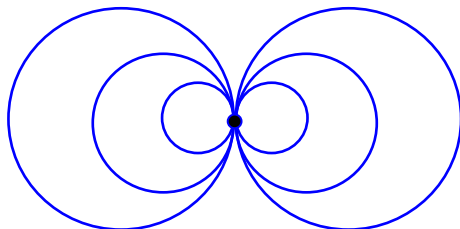
$$\frac{1}{\gamma(1 - \beta)} = 2\gamma$$

$$\omega_o = 2\gamma\omega_s$$

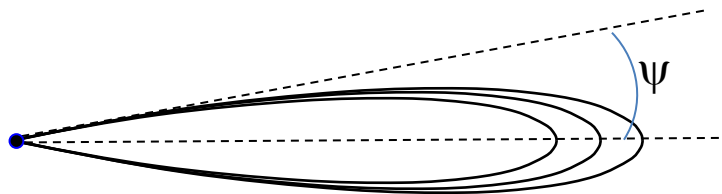
$$\lambda = \frac{\lambda'}{2\gamma}$$

For a beam of undulating electrons traveling at relativistic velocities toward the observer, the radiation frequency is upshifted by 2γ and the radiation cone narrows to an angle of $1/\gamma$

Radiation opening half-angle $\sim 1/\gamma$



Beam rest frame

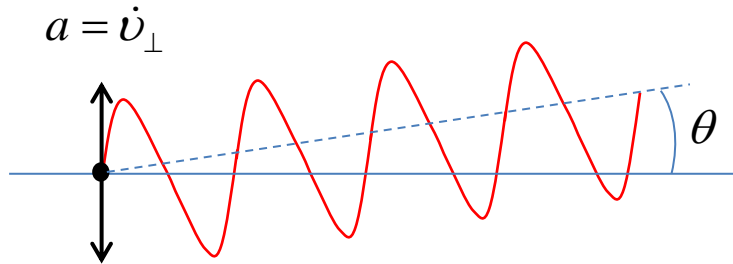


Lab frame

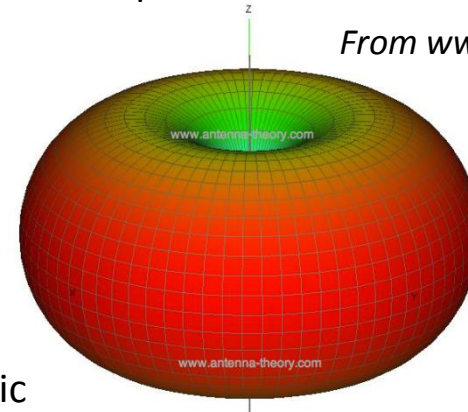
$$\psi = \frac{1}{\gamma}$$

Accelerated electrons radiate electromagnetic waves

Radio waves are produced when electrons are accelerated up and down an antenna



From www.antenna-theory.com



Power radiated per unit solid angle for non-relativistic electrons in circular orbits (a is perpendicular to v)

$$\frac{dP}{d\Omega} = \frac{e^2}{4\pi c} \frac{\sin^2(\theta) a^2}{c^2} \quad \xrightarrow{\text{Integrated over } \theta, \phi}$$

Larmor formula (cgs units)

$$P = \frac{2}{3} \frac{e^2 a^2}{c^3}$$

Relativistic generalization to the above equation increases the radiated power by a factor of γ^4 . Because of the γ^4 dependence, the power radiated by multi-GeV electrons is very high. This radiated power loss has to be replenished by klystron-driven RF accelerator cavities to maintain the same electron beam energy.

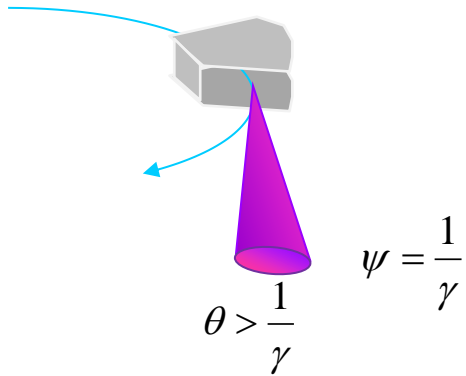
Liénard formula

$$P = \frac{2}{3} \frac{e^2 c}{\rho^2} \gamma^4$$

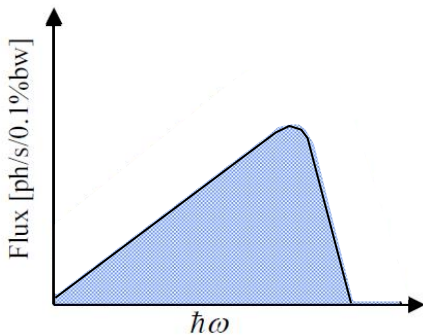
ρ is the orbit radius

Synchrotron Radiation Overview

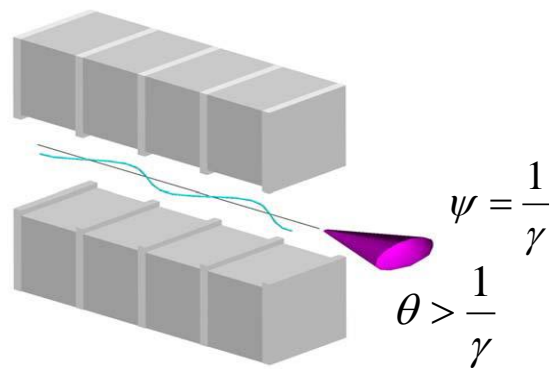
Bending magnet radiation



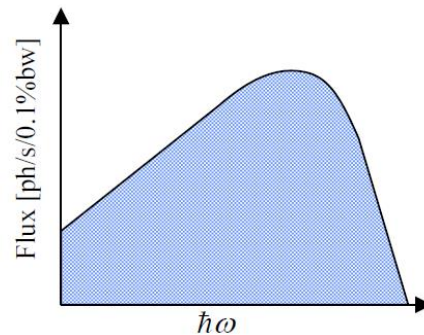
Broadband spectra
 Large angular distribution
 Low spectral brightness



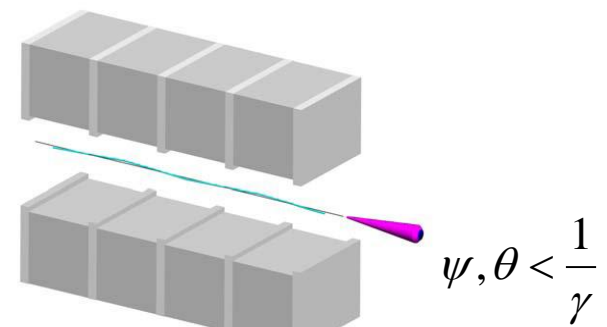
Wiggler radiation



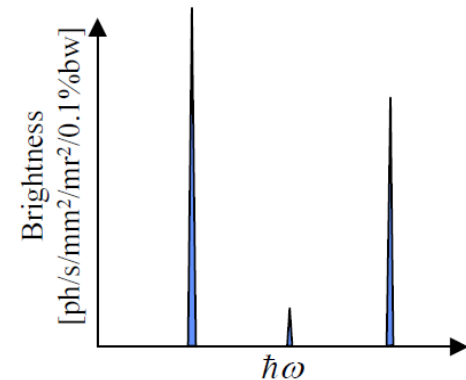
Broadband spectra
 Smaller angular distribution
 Higher spectral brightness



Undulator radiation

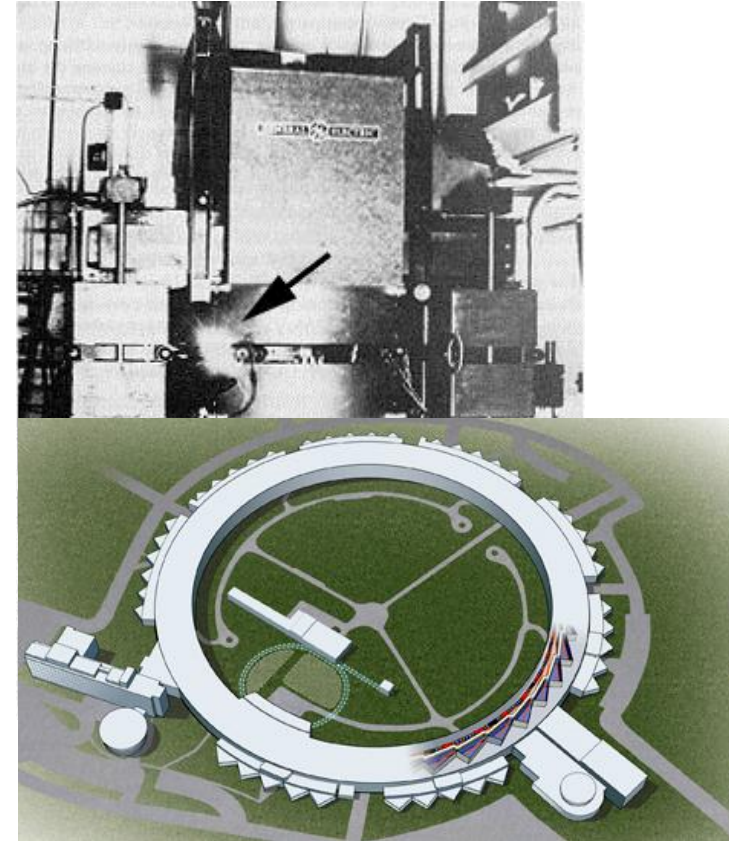


Narrow spectral peaks
 Highly collimated
 Highest spectral brightness

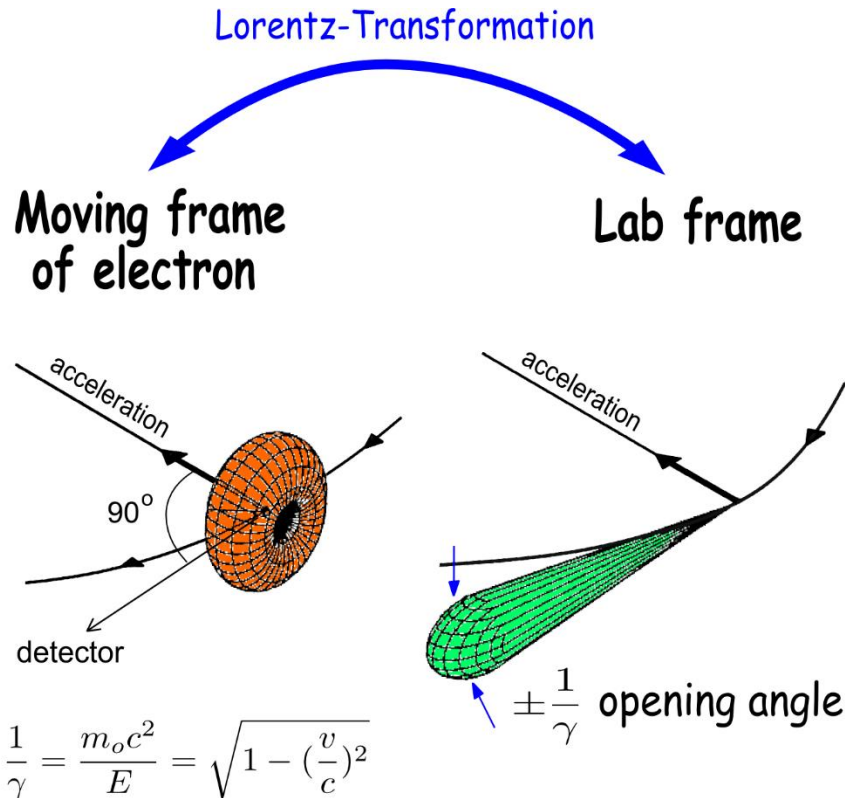


Four Generations of Light Sources

- 1st Generation Light Sources (storage rings)
 - Designed to accelerate electrons
 - SR first detected in GE 70-MeV synchrotron in 1947
- 2nd Generation Light Sources (storage rings)
 - Dedicated sources of synchrotron radiation
 - SPEAR2 became a dedicated light source in 1990
- 3rd Generation Light Sources (storage rings)
 - Low-emittance electron beams for high brightness
 - Straight sections to accommodate wigglers/undulators
 - Argonne Photon Source saw first light in 1995
- 4th Generation Light Sources (linac)
 - Coherent X-ray generation (N^2 radiation process)
 - Ultrafast (sub-ps to fs) X-ray pulses
 - Brilliance ten orders of magnitude higher than 3GLS
 - Linac Coherent Light Source at SLAC became the world's first hard X-ray FEL in 2008

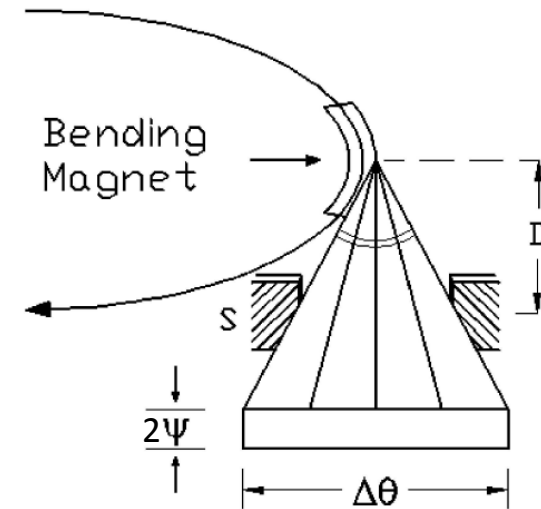


Bending Magnet Radiation 1



Example: 7 GeV electron beam

$$\psi = \frac{1}{\gamma} = \frac{1}{13700} \approx 73 \mu\text{rad}$$



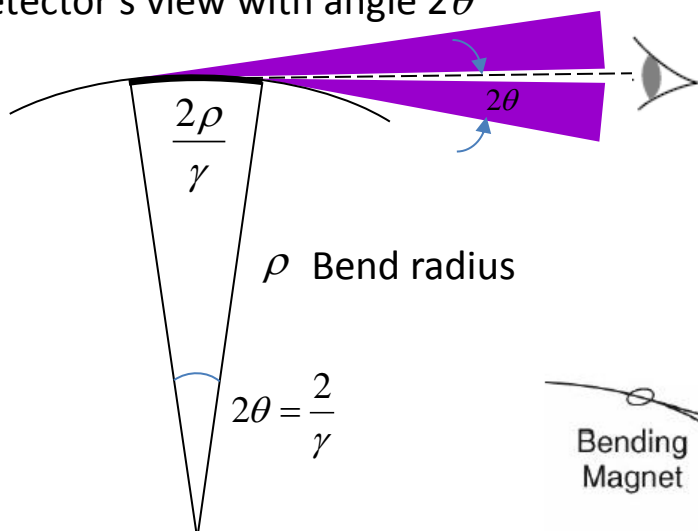
Vertical opening half-angle ψ is $1/\gamma$

Horizontal opening angle is large. The collection optics often limit the horizontal angle to ~ 1 mrad.

Radiation is linearly polarized in the orbital plane, and becomes elliptically polarized above/below orbital plane.

Bending Magnet Radiation 2

As a single electron traverses an arc within the detector's view with angle 2θ

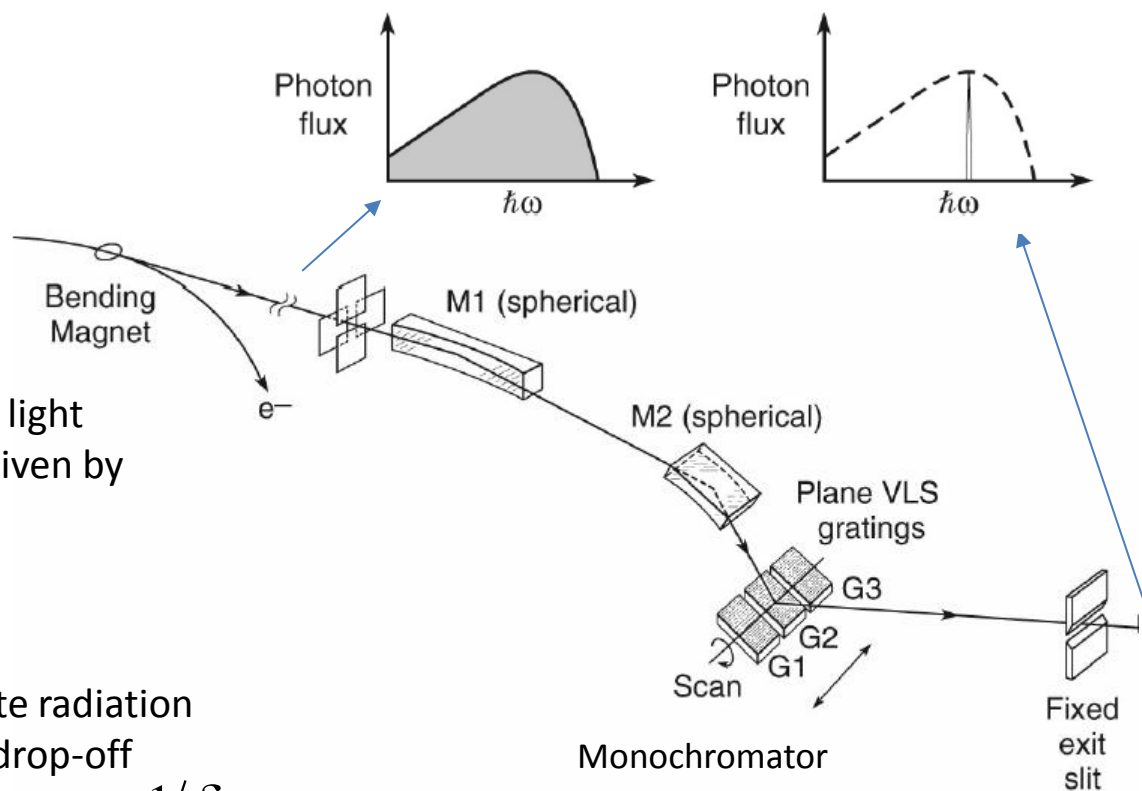


the detector measures an impulse of light with radiation time through the arc given by

$$\delta t \approx \frac{2\rho}{c\gamma} \left(\frac{1}{\beta} - 1 \right) \approx \frac{\rho}{c\gamma^3}$$

The Fourier transform of a short, finite radiation impulse is a broad spectrum up to a drop-off frequency called the critical frequency, $\omega_c \approx 1/\delta t$

Bending magnet radiation is often spectrally filtered to provide monochromatic radiation.



Bending Magnet Radiation

Critical photon energy

Critical photon energy

$$\varepsilon_c = \hbar\omega_c = \hbar \frac{3}{2} \frac{eB_0\gamma^2}{m_e}$$

Critical photon energy in practical units

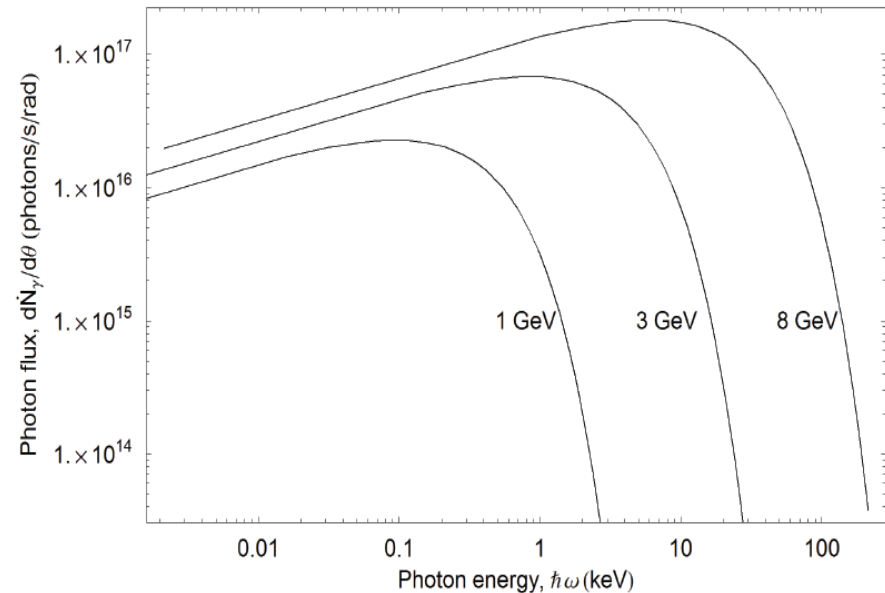
$$\varepsilon_c [keV] = 0.665 B_0 [T] E_b^2 [GeV]$$

Photon flux per unit angle (ph/s/mrad)

$$\frac{d\dot{N}_{ph}}{d\theta} \approx 4 \times 10^{16} E_b [GeV] I [A] \frac{\Delta\omega}{\omega} S\left(\frac{\omega}{\omega_c}\right)$$

Universal function

Photon flux of 1, 3, 8-GeV beam, B=0.5T I=1A



E_b (GeV)	Critical energy for $B=0.5T$ (keV)
1	0.33
3	3
8	21.3

Bending Magnet Radiation

Photon flux and universal function

Total photon flux, \dot{N}_{ph} = # of photons/s

By convention, only the photons within a bandwidth of **0.1%** of the central frequency and within an acceptance angle of **1 mrad** are used to compare the flux of different synchrotron radiation sources.

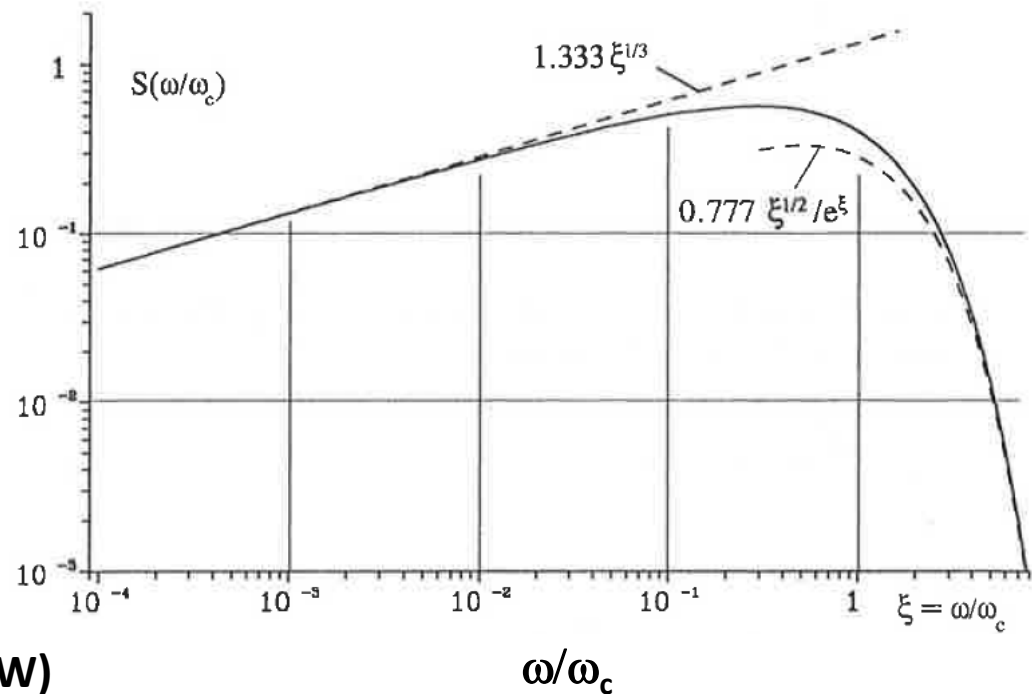
Spectral flux (ph/s/0.1% bandwidth)

$$F_s(\omega) = \frac{d\dot{N}_{ph}}{d\omega/\omega}$$

Spectral flux per θ (ph/s/mrad/0.1% BW)

$$\frac{dF_s(\omega)}{d\theta} = 4 \times 10^{13} E_b [GeV] I [A] S\left(\frac{\varepsilon}{\varepsilon_c}\right)$$

Universal function $S(\omega/\omega_c)$



Universal function relates the spectral flux to ratio of radiation frequency over the critical frequency. Universal function is independent of beam energy.

Plot from H. Wiedemann, "Particle Accelerator Physics II" Springer.

Synchrotron Radiation

Brilliance and emittance

Brilliance is defined as the number of photons per second per 0.1% bandwidth per unit solid angle per unit area. **Brilliance is conserved** for lossless systems.

Brilliance (ph/s/(mm-mrad)²/0.1% BW)

$$B = \frac{F_S(\omega)}{4\pi^2 \sigma_x \sigma_{x'} \sigma_y \sigma_{y'}} = \frac{F_S(\omega)}{4\pi^2 \varepsilon_x \varepsilon_y}$$

$F_S(\omega)$ = spectral flux in ph/s/0.1%

$\sigma_{x,y}$ = rms source size in x and y

$\sigma_{x',y'}$ = rms divergence angle in x and y

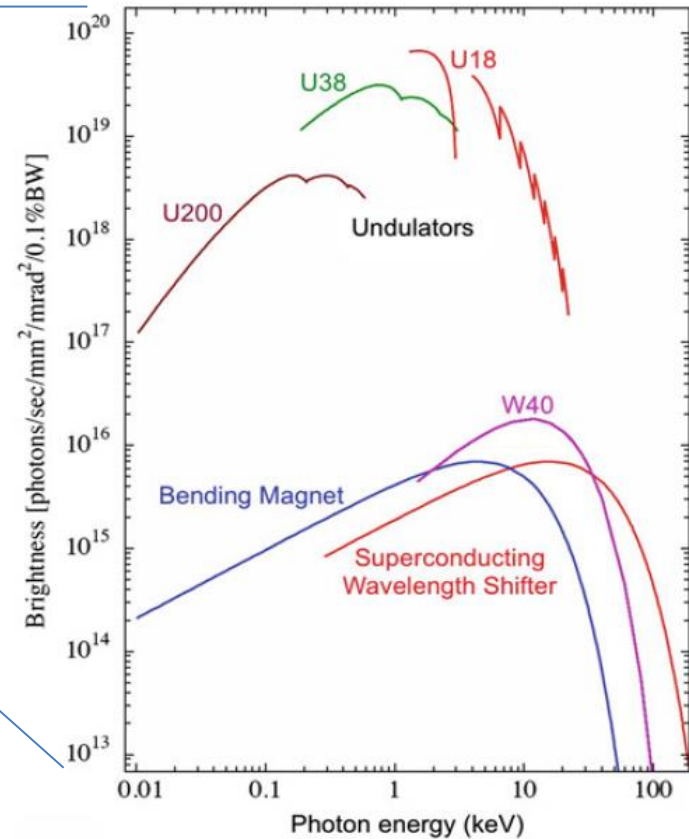
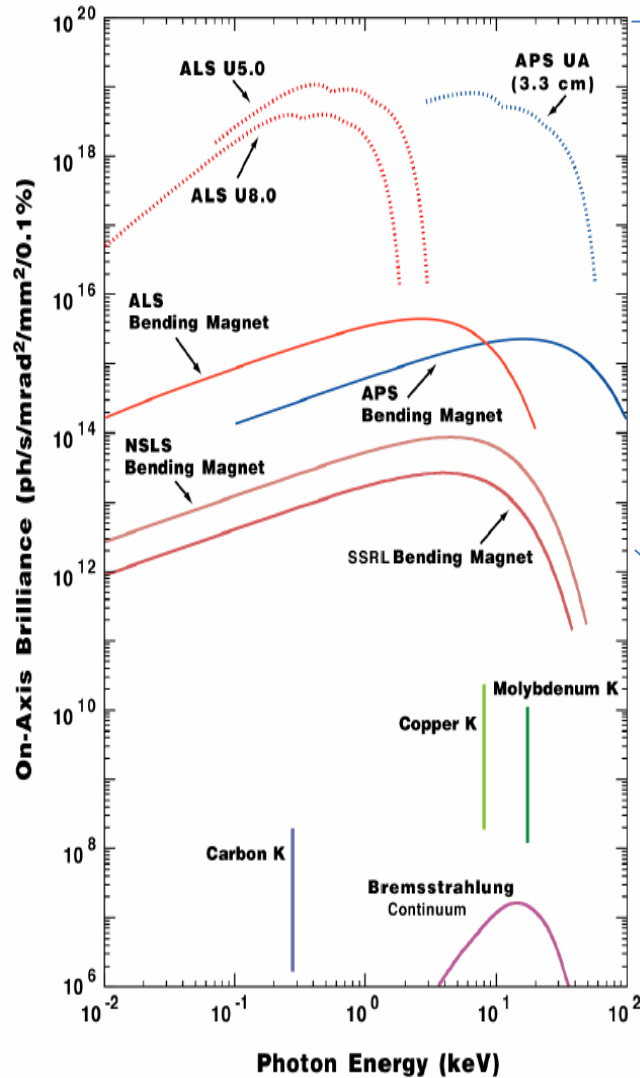
$\varepsilon_{x,y}$ = geometric emittance in x and y

The product of source size and divergence angle is the **geometric emittance** (in unit of mm-mrad), a measure of how small the electron beam can be focused to (σ_x, σ_y) and how collimated it is ($\sigma_{x'}, \sigma_{y'}$). At the beam waist, the geometric emittance is given by

$$\varepsilon_x = \sigma_x \sigma_{x'}$$

$$\varepsilon_y = \sigma_y \sigma_{y'}$$

Brilliance Comparison



Brilliance of undulator radiation is more than 10 orders of magnitude higher than the brilliance of X-ray tube Bremsstrahlung.

Beam Emittance in Rings

SR community unit = nm-rad (geometric) and mm-mrad (normalized)

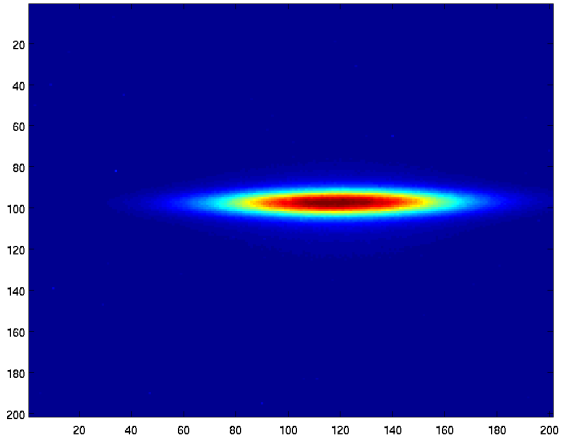
FEL community unit = nm (geometric) and μm (normalized)

Normalized emittance is γ times the **geometric emittance**

Example: typical geometric emittance at ALS

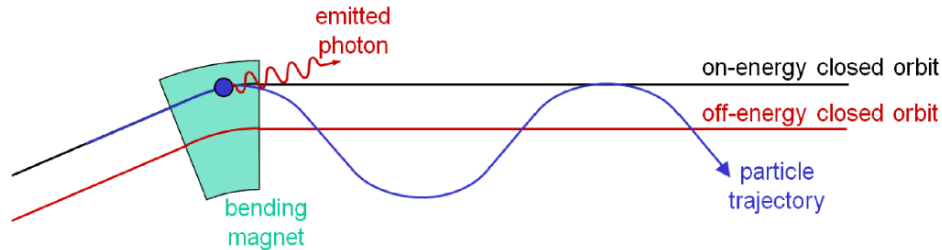
$$\varepsilon_x = 2\text{nm} - \text{rad}$$

$$\varepsilon_y \approx 0.04\text{nm} - \text{rad}$$



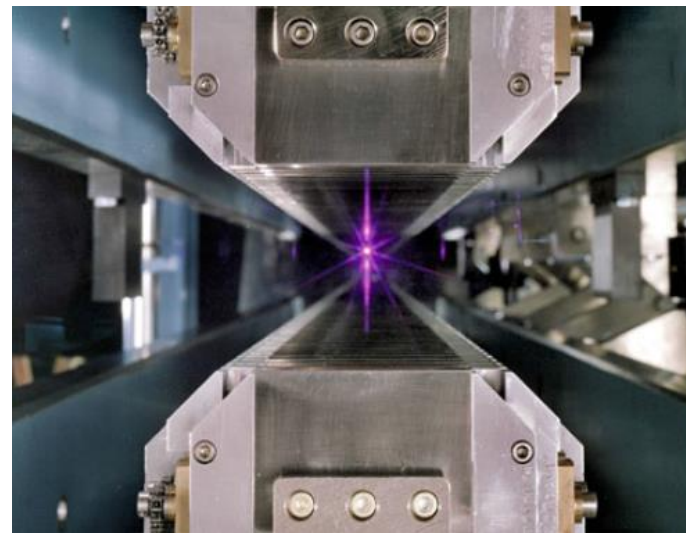
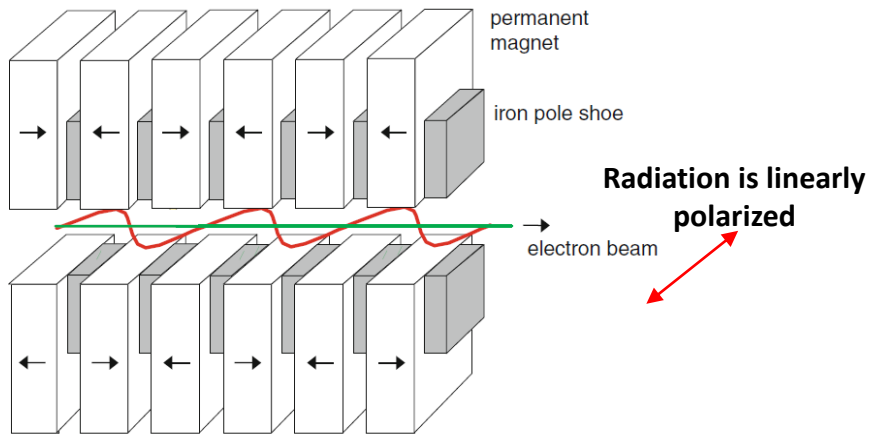
Electron momenta in all three directions are reduced as the electrons emit X-rays that carry away the photon momentum. As the longitudinal momentum p_z is restored with acceleration, the x and y emittances (ratios of p_x and p_y to p_z) are reduced (**radiation damping**).

Radiation damping is counteracted by the **quantum excitation** due to random changes in the electron orbit around the ring. The **equilibrium emittance** in x is larger than the emittance in y .

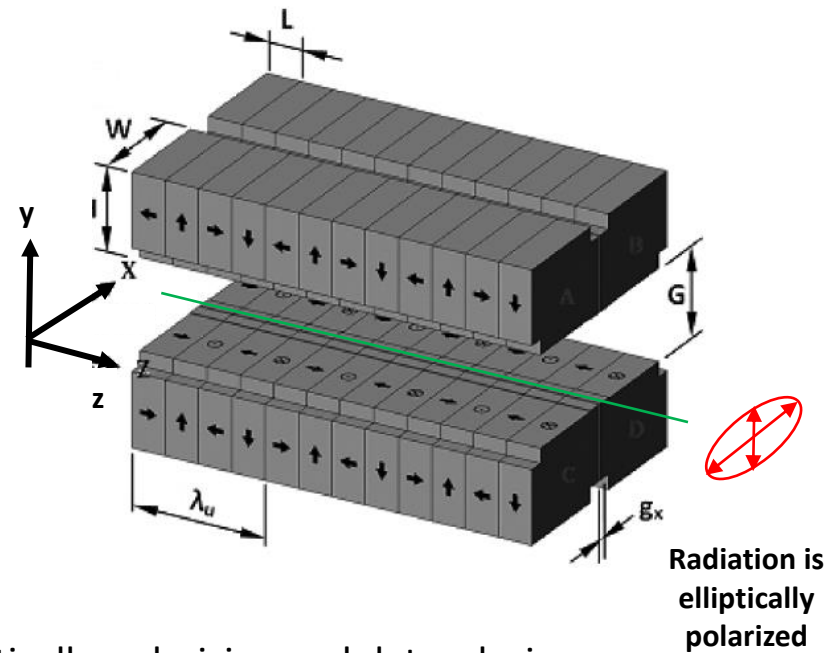


Insertion Devices

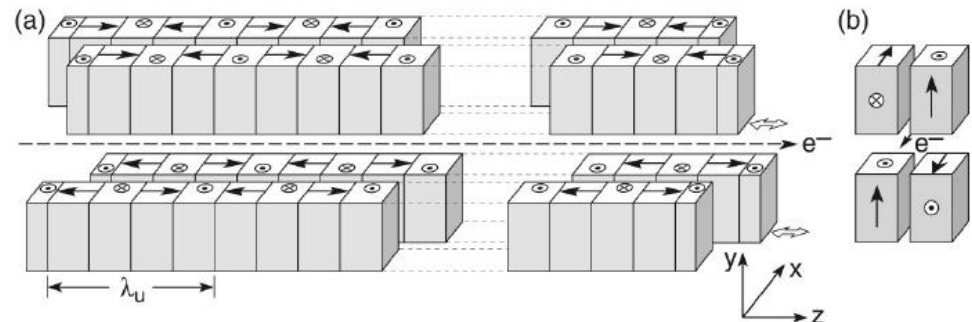
Plane-polarized wiggler/undulator



Elliptically-polarizing undulator



An elliptically-polarizing undulator design



Electron Motion in a Wiggler/Undulator

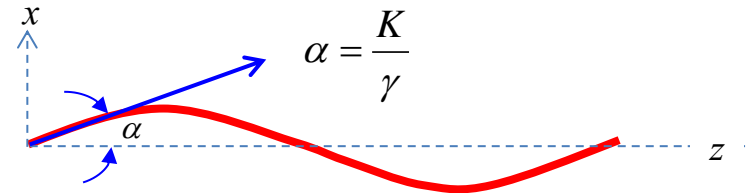
Magnetic field $B_y = -B_0 \sin(k_u z)$

Force $\gamma m_e \dot{\mathbf{v}} = -e\mathbf{v} \times \mathbf{B}$

Acceleration $a_x = \ddot{x} = \frac{ec}{\gamma m_e} B_y$

Transverse velocity $v_x = \frac{c}{\gamma} \frac{eB_0}{m_e c k_u} \cos(k_u z)$

Transverse motion $x = \frac{K}{k_u \gamma} \sin(k_u z)$



K is a measure of the angle the electrons make relative to $1/\gamma$ as it crosses the z axis

Dimensionless undulator parameter K

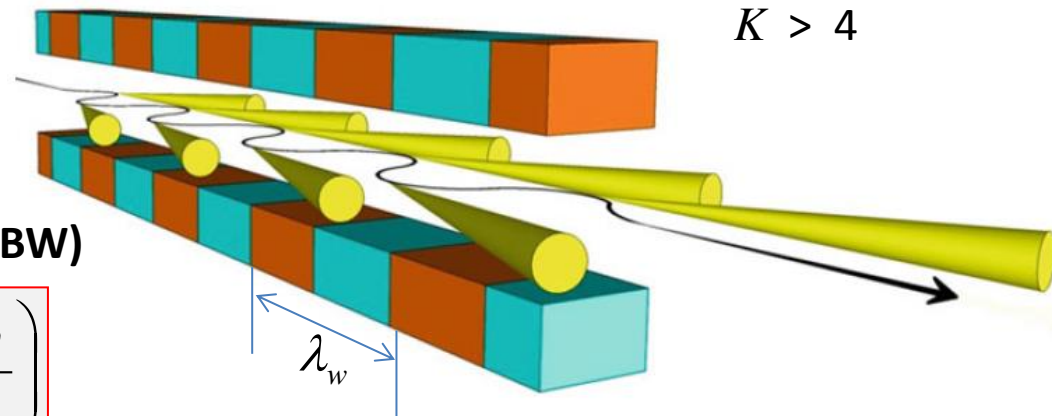
$$K = \frac{eB_0}{m_e c k_u}$$

In practical units, K is given by

$$K = 0.934 \lambda_u [cm] B_0 [T]$$

Wiggler Radiation

Radiation from a **multi-pole wiggler** with N_w periods adds up incoherently to give $2N_w$ times the bending magnet radiation.



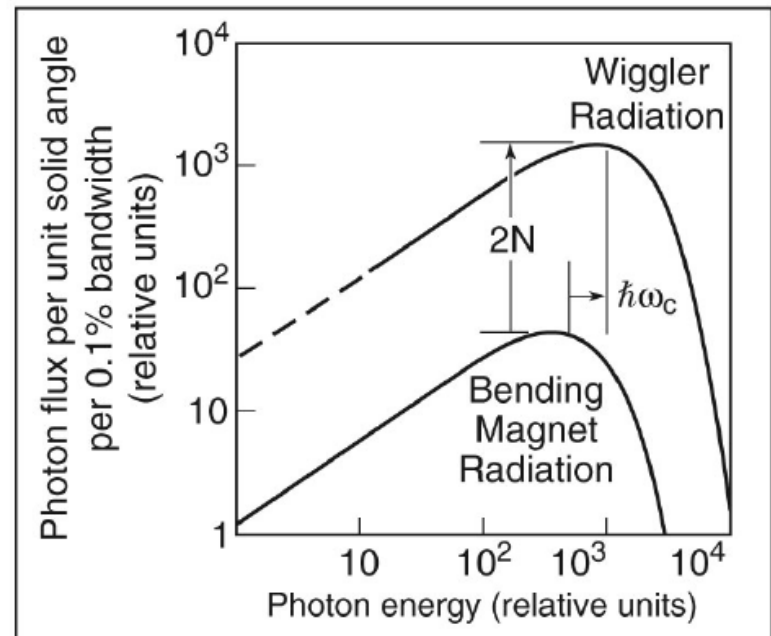
Spectral flux per θ (ph/s/mrad/0.1% BW)

$$\frac{dF_s}{d\theta} = 8 \times 10^{13} N_w E_b [GeV] I [A] S \left(\frac{\omega}{\omega_c} \right)$$

Total wiggler power

$$P [kW] = 0.633 E_b^2 [GeV] I [A] B_0^2 [T] L [m]$$

Wiggler magnetic fields are higher than the fields of bending magnets, so the critical photon energy is shifted to higher energy. Superconducting **wavelength shifters** can achieve photon energies above 100 keV.



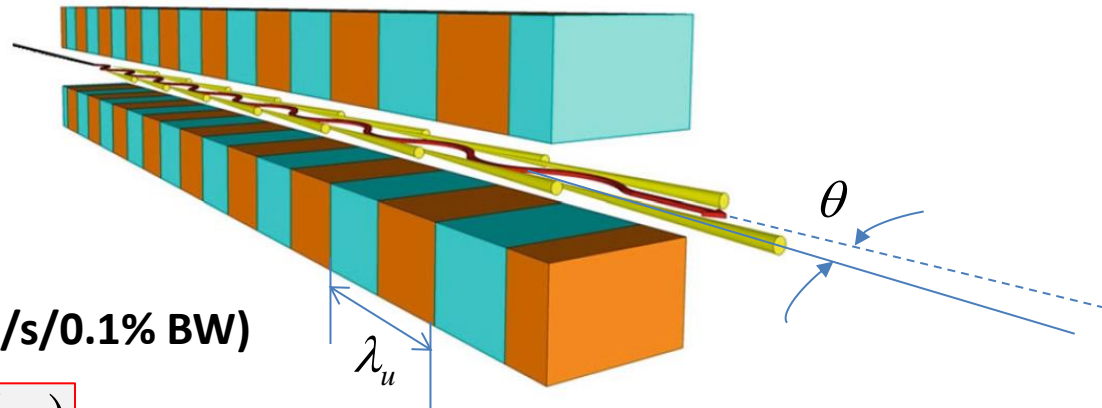
Undulator Radiation

Wavelength of the n^{th} harmonic

$$\lambda_n = \frac{\lambda_u}{2n\gamma^2} \left(1 + \frac{K^2}{2} + \gamma^2 \theta^2 \right)$$

Undulator radiation spectral flux (ph/s/0.1% BW)

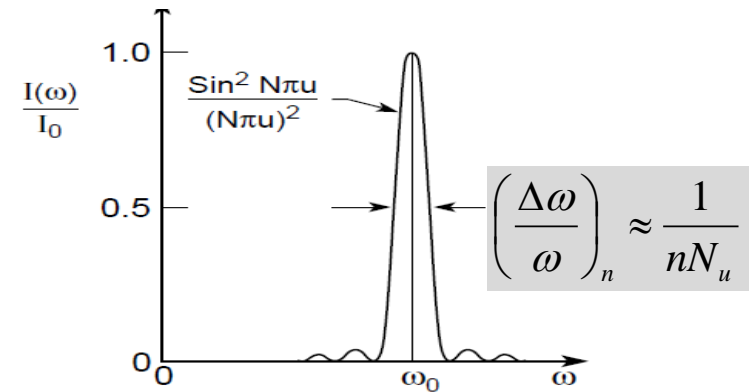
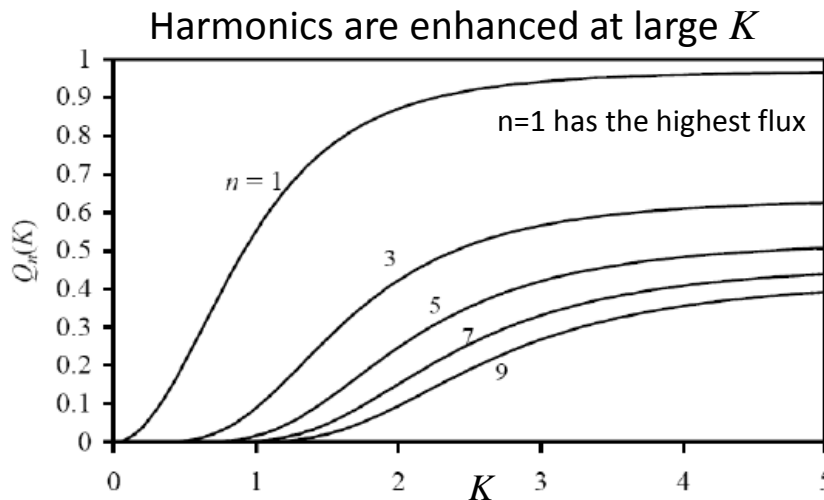
$$S(n, K) = 1.43 \times 10^{14} N_u I[A] Q_n(K)$$



Interference of the electric fields from $2N_u$ radiation cones gives rise to narrowing of

- fundamental cone angle
- spectral distribution

$$\theta = \frac{1}{\gamma \sqrt{N_u}}$$



Undulator Radiation Harmonics

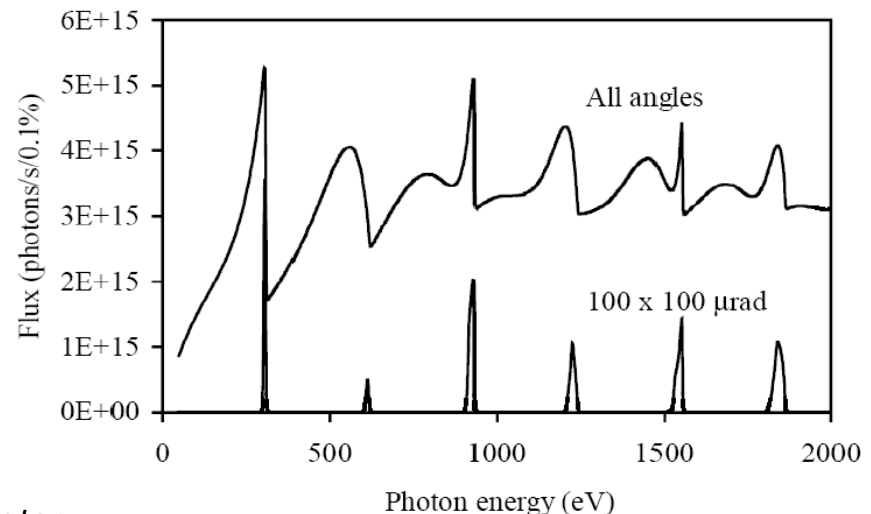
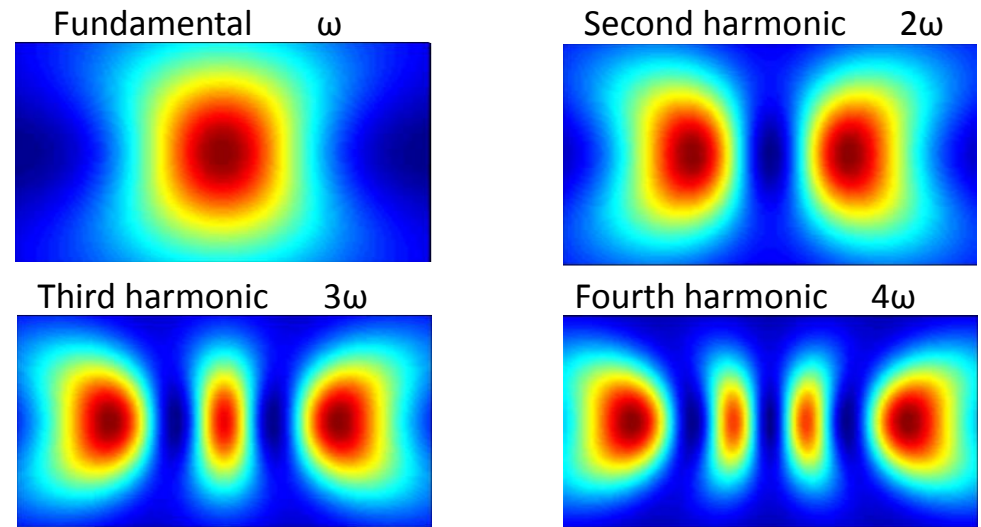
Undulator radiation is polarized in the horizontal direction for a plane-polarized undulator. The vertical opening angle is

$$\psi = \frac{1}{\gamma \sqrt{N_u}}$$

The horizontal angle of the central lobe(s) becomes narrower at the higher harmonics.

$$\theta_n = \frac{1}{n\gamma \sqrt{N_u}}$$

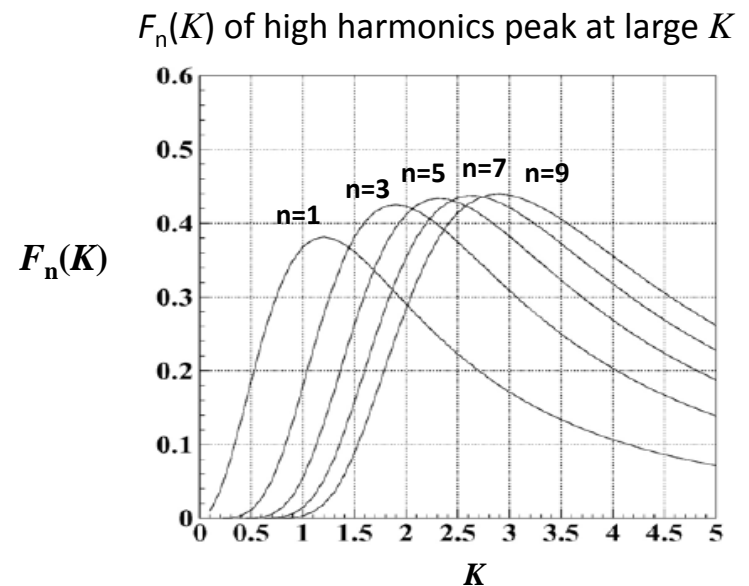
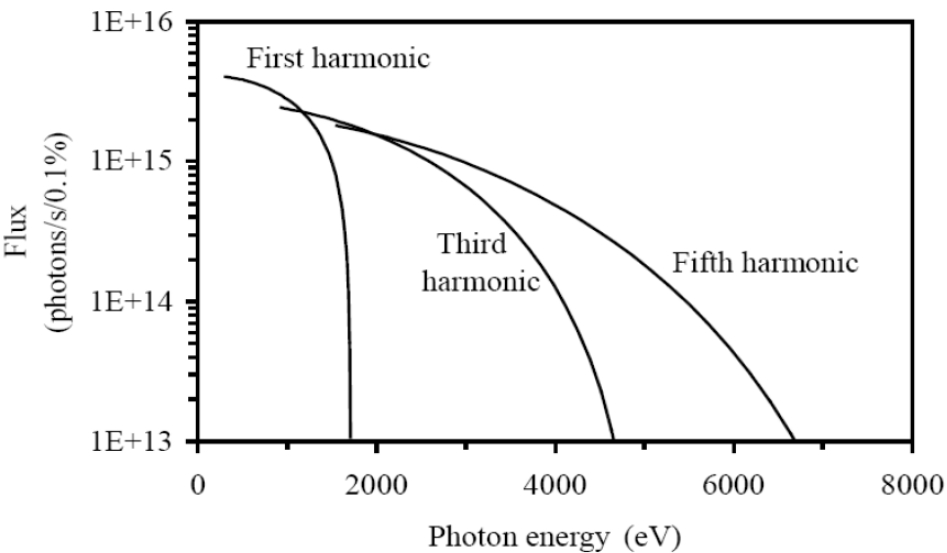
Viewed along the axis, the odd harmonics have both on- and off-axis lobes. The even harmonics have off-axis lobes only. As the aperture size is reduced, the low-energy shoulder and the even harmonics are clipped off.



Undulator K and Tuning Curves

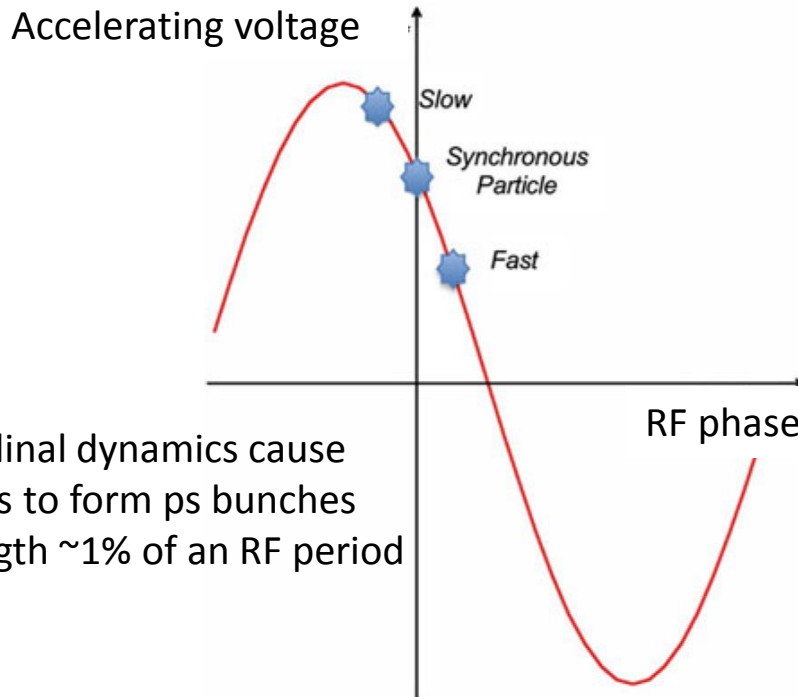
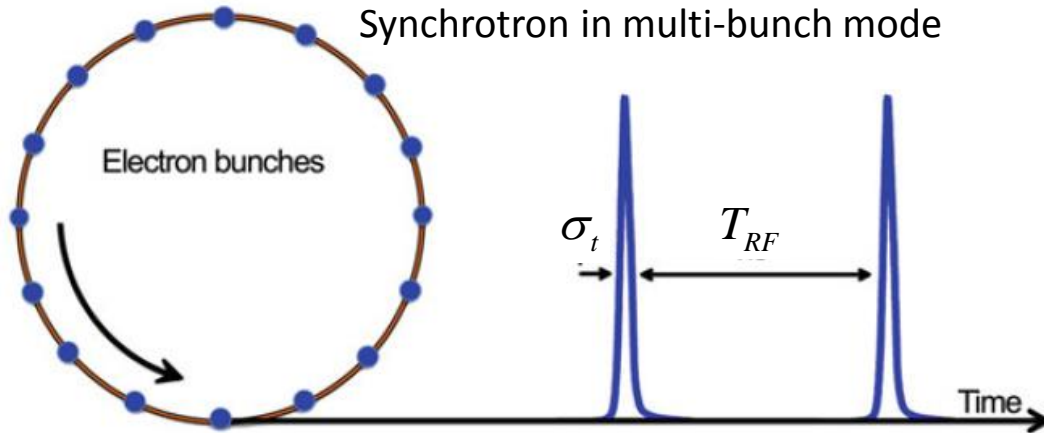
On-axis Brightness (ph/s/mrad²/0.1% BW)

$$I_n = \frac{dS(n, K)}{d\Omega} = 1.74 \times 10^{14} N_u^2 E_b^2 [GeV] I [A] F_n(K)$$



The undulator tuning curves are obtained by opening/closing the undulator gap, thereby decreasing/increasing the undulator K parameter. The left points of the tuning curves correspond to maximum K (smallest gap) and the right correspond to minimum K (largest gap).

Synchrotron Radiation Pulse Format



Longitudinal dynamics cause electrons to form ps bunches with length $\sim 1\%$ of an RF period

RF period (min. bunch spacing)

$$T_{RF} = \frac{1}{f_{RF}}$$

Max. # of bunches in ring

$$N_b = \frac{C f_{RF}}{c}$$

rms bunch length

$$\sigma_t \approx 0.01 T_{RF}$$

Peak / average flux (multi-bunch)

$$\frac{F_{pk}}{F_{av}} = \frac{T_{RF}}{\sigma_t} \approx 10^2$$

Major Synchrotron Radiation Facilities in the US



Advanced Light Source (ALS) at Lawrence Berkeley National Lab



Argonne Photon Source (APS) at Argonne National Lab

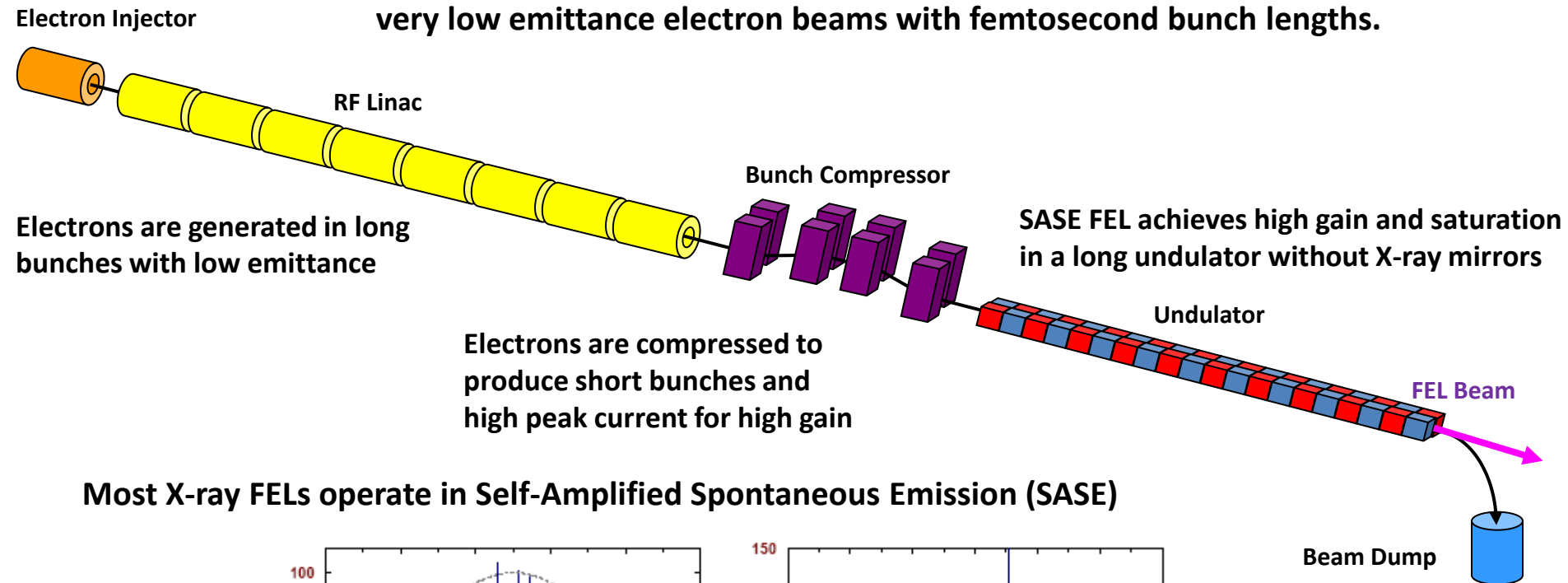


National Synchrotron Light Source II (NSLS-II) at Brookhaven National Lab

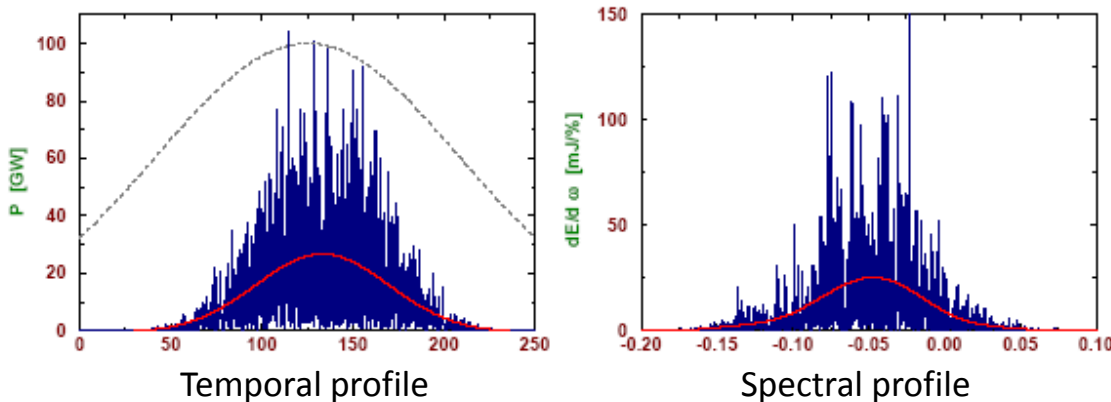
	ALS		APS		NSLS-II	
Nominal and max. electron beam energy	1.5 GeV 1.9 GeV		7 GeV 7.5 GeV		3 GeV	
Ring circumference	196.8 m		1,104 m		791.5 m	
Current	400 mA		100 mA		500 mA	
Critical photon energy	1.53 keV @ 1.5 GeV		19.5 keV @ 7 GeV		2.4 keV @ 3 GeV	
Min. bunch spacing Max. #bunches in ring	2 ns 328		2.84 ns 1296		2 ns 1320	
Bunch length, rms	15 - 40 ps		~22 ps		10 ps	
Horizontal/vertical emittance	2.0 nm	0.04 nm	3.1 nm	0.001 nm	0.9 nm	0.008 nm

Linac-driven X-ray FEL

Linac-driven XFEL are single-pass devices driven by high-energy (~ 10 GeV), very low emittance electron beams with femtosecond bunch lengths.



Most X-ray FELs operate in Self-Amplified Spontaneous Emission (SASE)

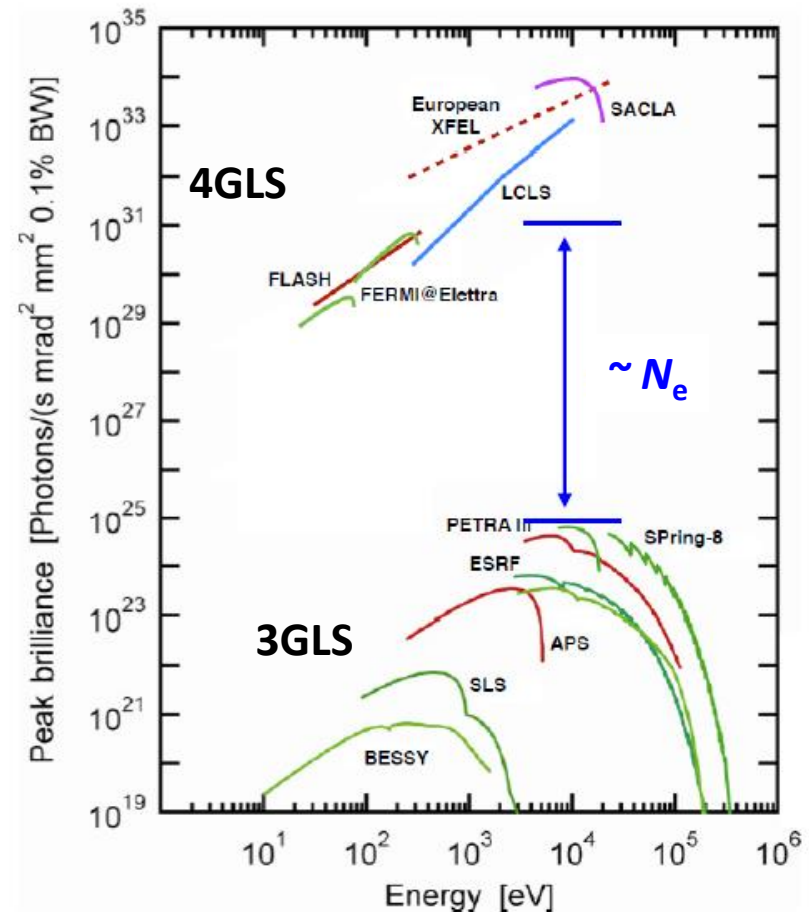


3GLS and 4GLS Comparison

Peak brilliance (ph/s/mm²/mrad²/0.1% BW)

$$B_{pk} = \frac{N_{ph}}{4\pi^2 \varepsilon_x \varepsilon_y \Delta t (\Delta\omega/\omega)}$$

	3GLS UR	4GLS	Ratio
N_{ph}	10^8	10^{12}	10^4
ε_x	2 nm	.02 nm	10^2
ε_y	.02 nm	.02 nm	1
Δt	~30 ps	~30 fs	10^3
$\Delta\omega/\omega$	1%	0.1%	10
B_{pk}	10^{23}	10^{33}	10^{10}



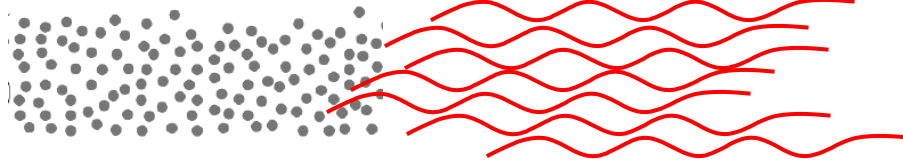
However, 3GLS can deliver higher average brilliance X-ray beams (at high pulse repetition rates) to multiple users simultaneously, whereas 4GLS can deliver beams to only 1-2 users presently.

Bunched Beam Radiation

A single electron emitting radiation wavelet with electric field amplitude \mathcal{E}



Ensemble of randomly distributed electrons



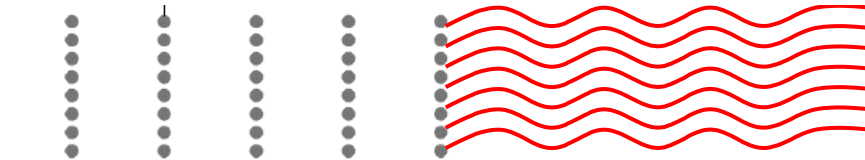
Each electron generates its own electric field. The sum of N_e wavelets with random phases is proportional to square root of N_e .

Incoherent radiation



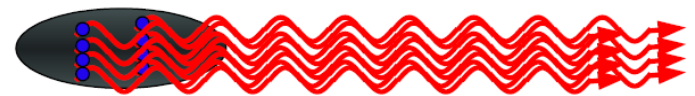
$$|E| = \sqrt{N_e} |\mathcal{E}| \quad I = N_e |\mathcal{E}|^2$$

Ensemble of bunched electrons with λ period



The sum of N_e wavelets is proportional to N_e .
The intensity is proportional to N_e^2 .

Coherent bunched beam radiation

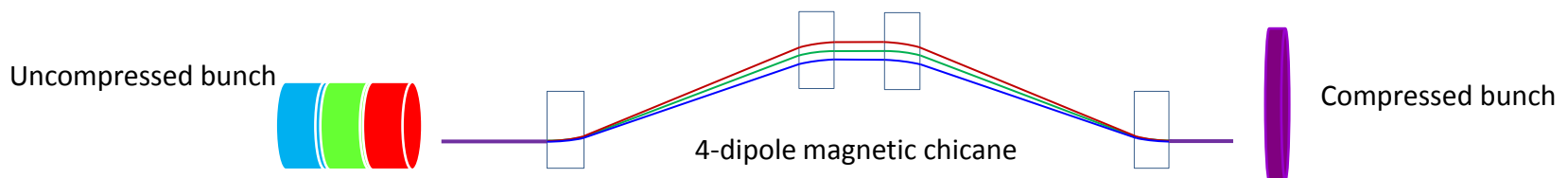
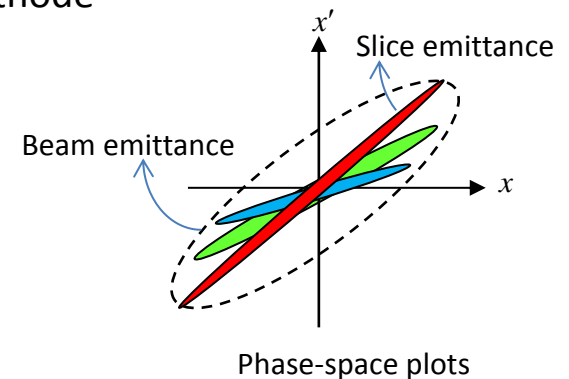


$$|E| = N_e |\mathcal{E}| \quad I = N_e^2 |\mathcal{E}|^2$$

N_e is the number of electrons

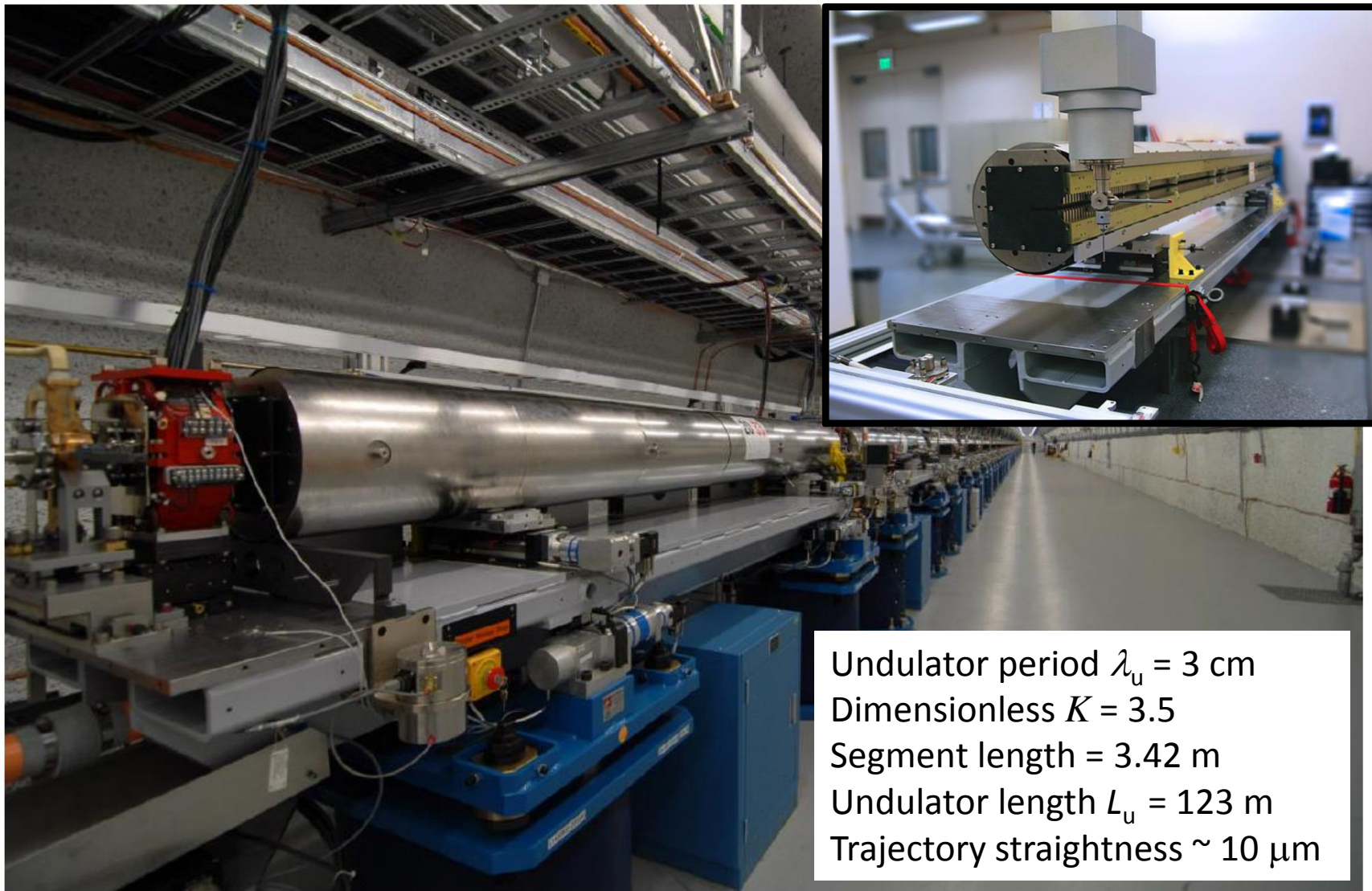
Enabling Technologies for XFEL

- Low-emittance electron **photoinjectors**
 - Electron bunches are produced from a laser-gated photocathode
 - Phase space ellipses oscillate about equilibrium
 - Solenoid fields align the ellipses, reduce beam emittance
 - Slice emittance is more relevant to XFEL performance
- High-brightness electron linac
 - Electrons are matched into accelerator cavities
 - **Phase-space oscillation** is damped with acceleration
- Electron **bunch compression**
 - Electron bunches are compressed to generate kA peak current



- High current leads to high gain, but causes electrons to undergo coherent synchrotron radiation (CSR) and microbunch instabilities (μ BI) that are bad for XFEL.
- Modern linac designs balance non-linear effects to produce **high-peak-current, small-emittance, low-energy-spread electron beams.**

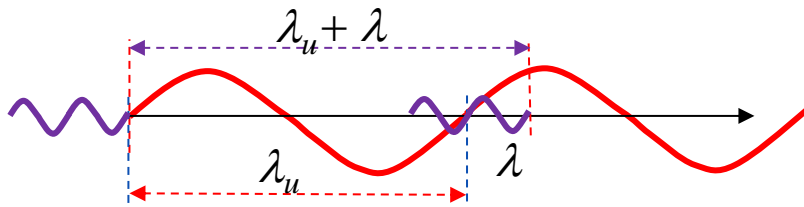
Linac Coherent Light Source Undulator



Undulator period $\lambda_u = 3$ cm
Dimensionless $K = 3.5$
Segment length = 3.42 m
Undulator length $L_u = 123$ m
Trajectory straightness ~ 10 μ m

Resonant Wavelength

At resonance, the radiation pulse slips ahead of electrons one wavelength every period



In the time the electron (red) traverses one undulator period, the radiation wave (purple) traverses 1 undulator period plus 1 wavelength.

$$t = \frac{\lambda_u}{\bar{v}_z} = \frac{\lambda_u + \lambda}{c}$$

$$\frac{\lambda}{\lambda_u} = \frac{c}{\bar{v}_z} - 1$$

$$\frac{\lambda}{\lambda_u} = \frac{1}{1 - \frac{1}{2\gamma^2} \left(1 + \frac{K^2}{2} \right)} - 1$$

$\underbrace{\hspace{10em}}_{\bar{v}_z}$

FEL Resonant Wavelength

$$\lambda = \frac{\lambda_u}{2\gamma^2} \left(1 + \frac{K^2}{2} \right)$$

The **average axial velocity** is slower than βc because of the average transverse velocity.

$$\bar{v}_z^2 = (\beta c)^2 - \bar{v}_x^2$$

How does an FEL work?

Resonance condition

- Radiation slips over electrons one λ after each λ_u
- Ponderomotive phase (radiation phase + electron phase) is constant
- This allows electrons and radiation to exchange energy continuously

Energy modulation

- Electrons with ponderomotive phase between $-\pi$ and 0 gain energy
- Electrons with ponderomotive phase between 0 and $+\pi$ lose energy
- This leads to energy modulations with a period of the radiation wavelength

Density modulation

- Electrons that gain energy move forward in phase
- Electrons that lose energy move back in phase
- This leads to density modulations with a period of the radiation wavelength
- Harmonic current amplifies the radiation which then causes even more bunching

Coherent radiation

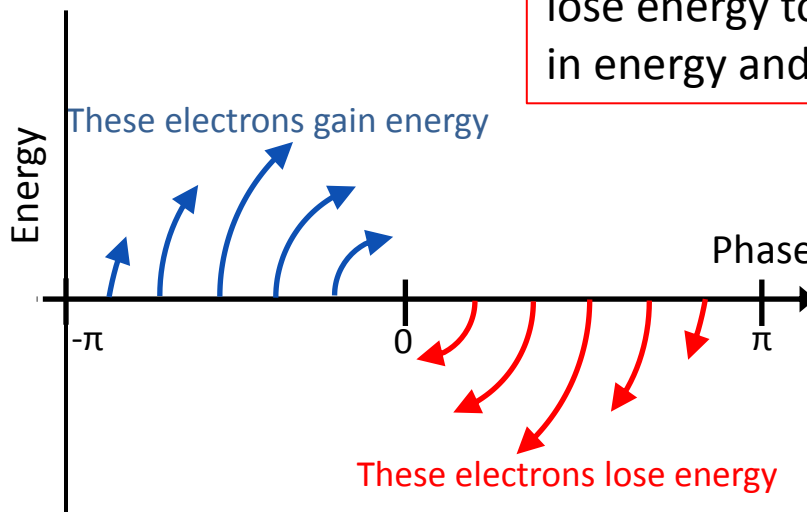
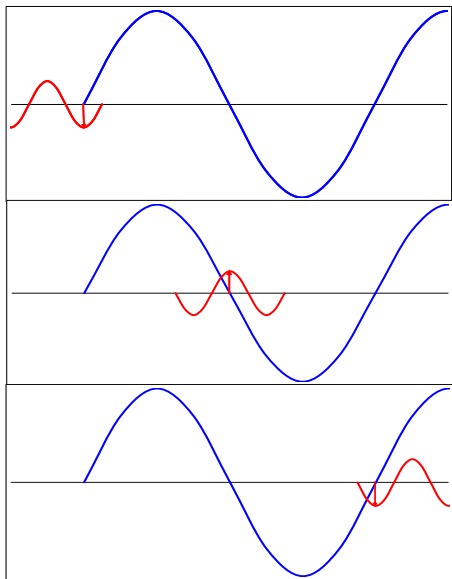
- Density-modulated electrons radiate coherently
- Radiation intensity scales with N_e^2 (increased by N_e over undulator radiation)

Energy Exchange in FEL

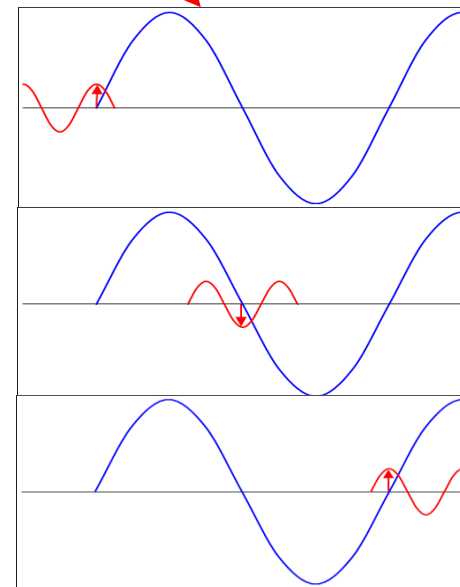
The rate of energy exchange depends on the dot product of **transverse electron current** and **radiation electric field**

$$\dot{W} = \mathbf{j}_{\perp} \cdot \mathbf{E}_r$$

The electrons with ponderomotive phase between 0 and $\pi/2$ continuously lose energy to the radiation; move down in energy and to the left in phase.

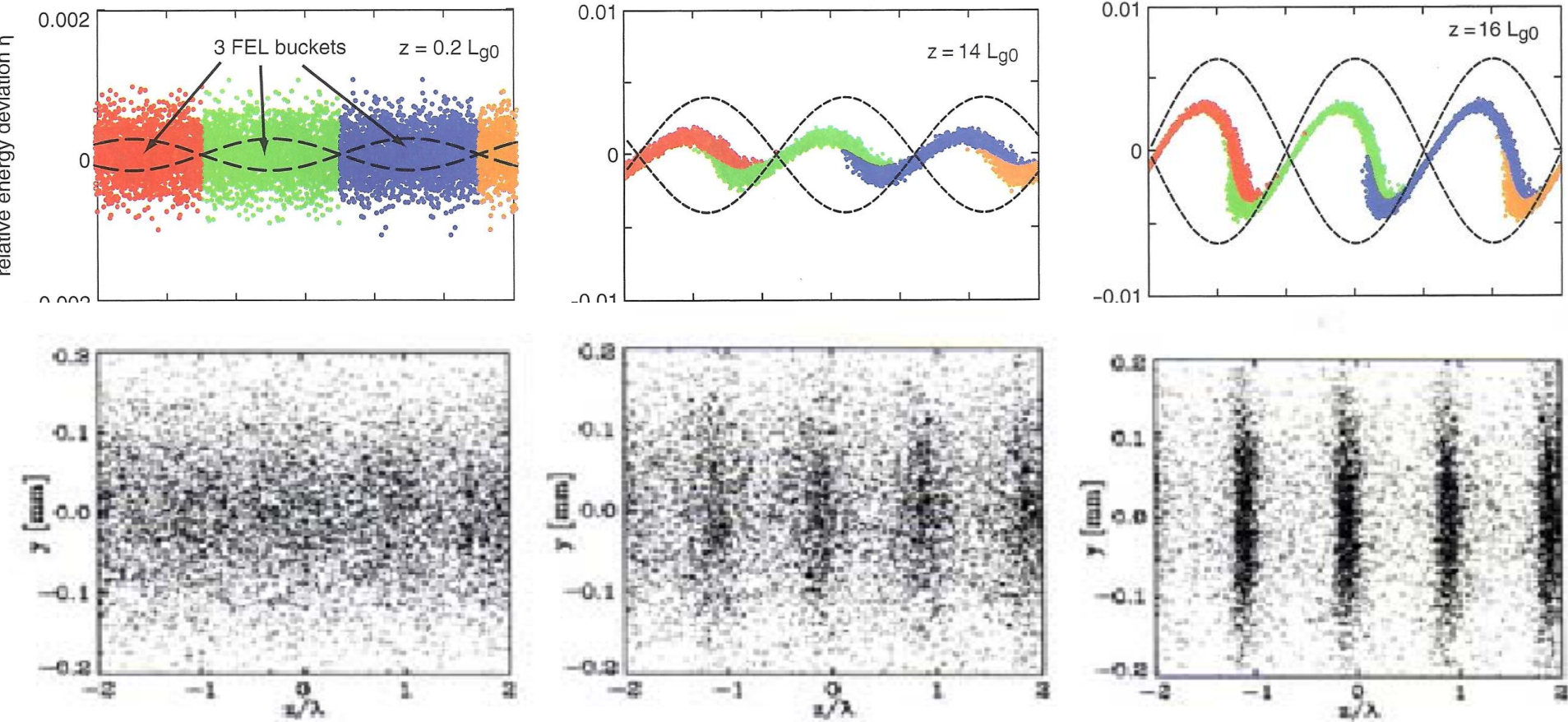


The electrons with ponderomotive phase between $-\pi/2$ and 0 continuously gain energy from the radiation; move up in energy and to the right in phase.



Energy Modulation & Microbunching

Initially unbunched beams develop energy and density modulations (microbunching).



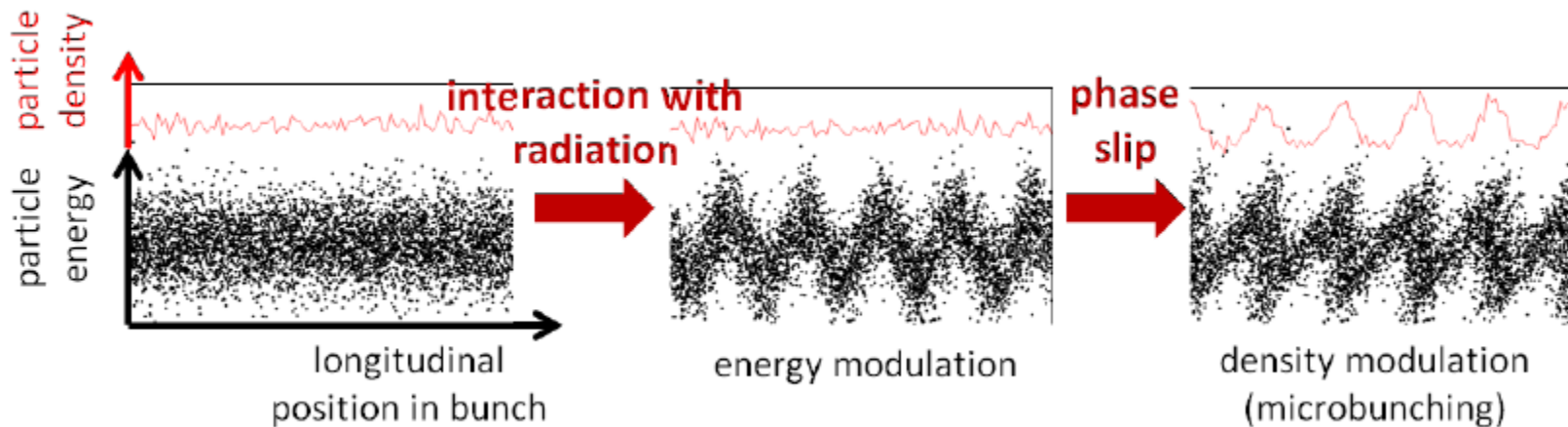
At entrance to the undulator

Exponential gain regime

Saturation(maximum bunching)

Graphics from "Ultraviolet and Soft X-ray Free-Electron Lasers" by P. Schmüser, M. Dohlus and J. Rössbach

Coherent Radiation from Microbunched Electrons



Unbunched beams produce undulator radiation with random phases, large phase errors.

Microbunched beams produce coherent radiation with small phase errors.

Electric field of N random electrons

$$E_T = \sum_n^N E_0 e^{i\phi_n}$$

Electric field of N microbunched electrons

$$|E_T| = \sqrt{N} |E_0|$$

$$|E_T| = N |E_0|$$

Undulator radiation power

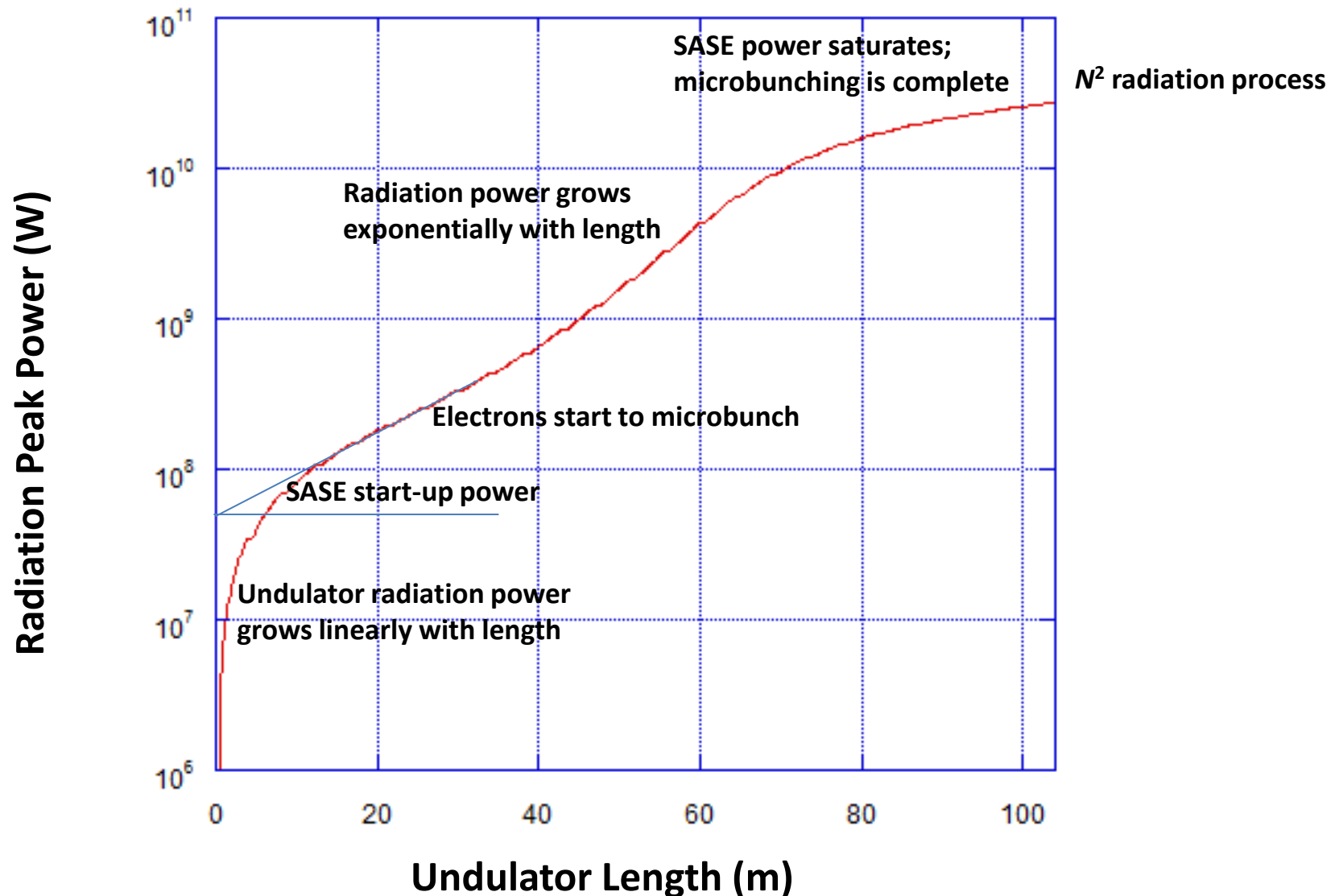
FEL power (N^2 process)

$$P_T = N p_e$$

$$P_T = N^2 p_e$$

Graphics courtesy of A. Wolski, "A Short Introduction to Free-Electron Lasers," CAS 2012

Self-Amplified Spontaneous Emission



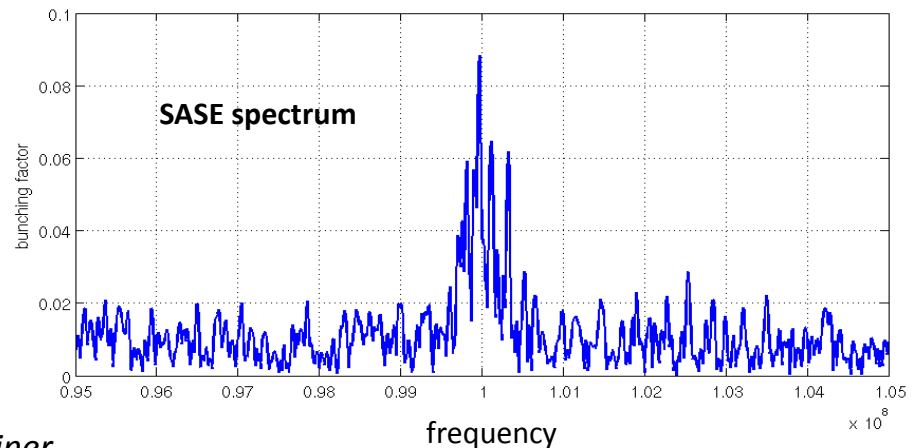
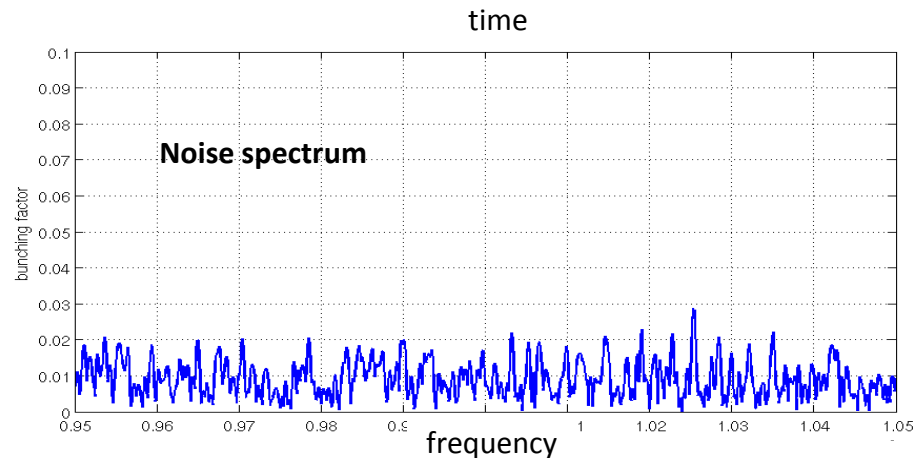
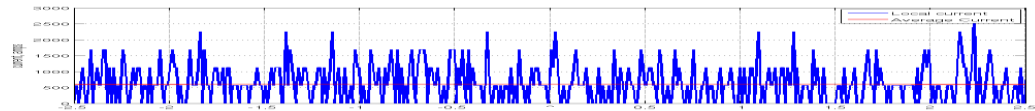
SASE Start-up Noise

Discreteness of electrons leads to random fluctuations in current.



Taking the Fourier transform of current fluctuations, one gets frequency dependent random bunching as a function of frequency.

The FEL amplifies a narrow portion of the initial SASE seed within the FEL gain bandwidth. As this portion starts from noise, the random and chaotic nature of the initial bunching is still visible in the amplified FEL radiation.



SASE power starts from noise; pulse energy fluctuates from shot to shot

Power grows exponentially with length

$$P(z) \approx \frac{P_{noise}}{9} \exp\left(\frac{z}{L_G}\right)$$

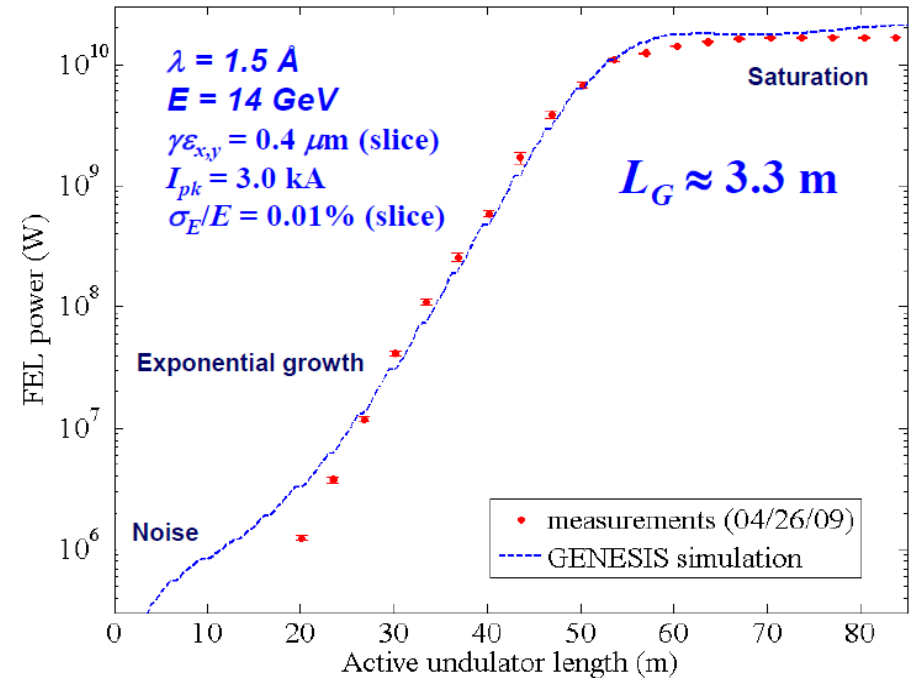
Power gain length

$$L_G = \frac{\lambda_u}{4\pi\sqrt{3\rho}}$$

FEL power at saturation (at $\sim 20 L_G$)

$$P_S = \rho \frac{I_{pk} E_b}{e}$$

Increase rho \rightarrow higher gain (shorter gain length) and higher saturation power. Typical rho for XFEL ~ 0.0005 (0.05%).

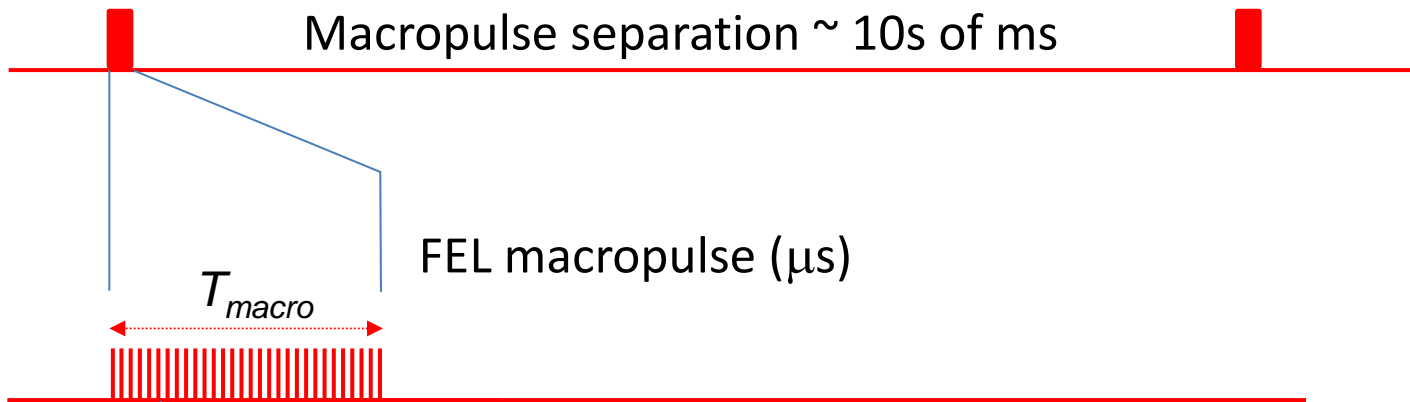


FEL rho parameter

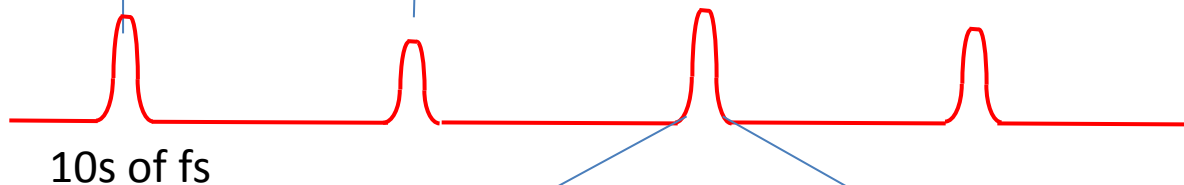
$$\rho = \frac{1}{\gamma} \left(\frac{K\lambda_u}{8\pi\sigma_b} \right)^{\frac{2}{3}} \left(\frac{I_{pk}}{I_A} \right)^{\frac{1}{3}}$$

Linac-driven SASE Pulse Format

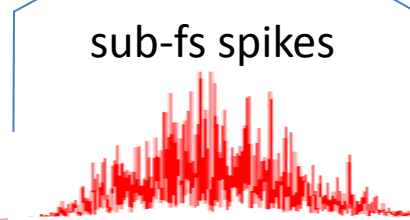
RF macropulses



FEL micropulses (bunches)

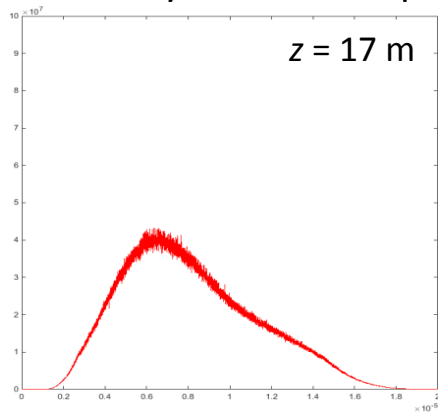


Each micropulse has a different set of spikes and pulse energy

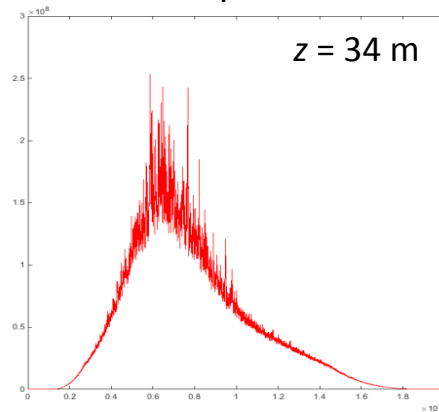


SASE Spikes Formation

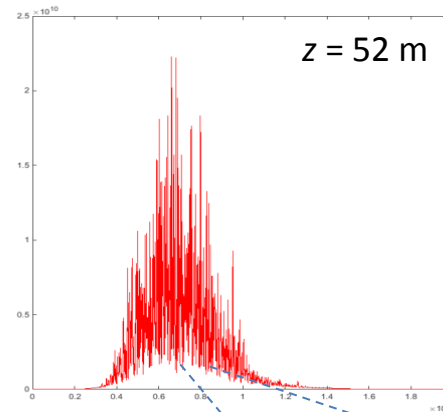
Intensity versus time plots at different positions along the undulator



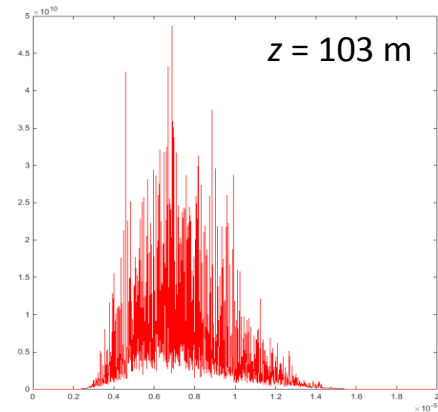
Initial radiation pulse resembles current profile.



SASE spikes start to appear in exponential growth regime.



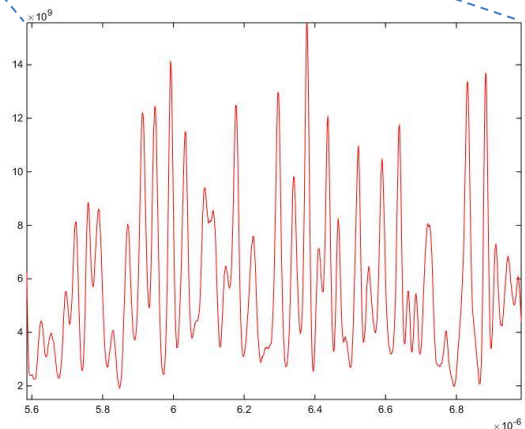
At saturation, SASE spikes have the longest length.



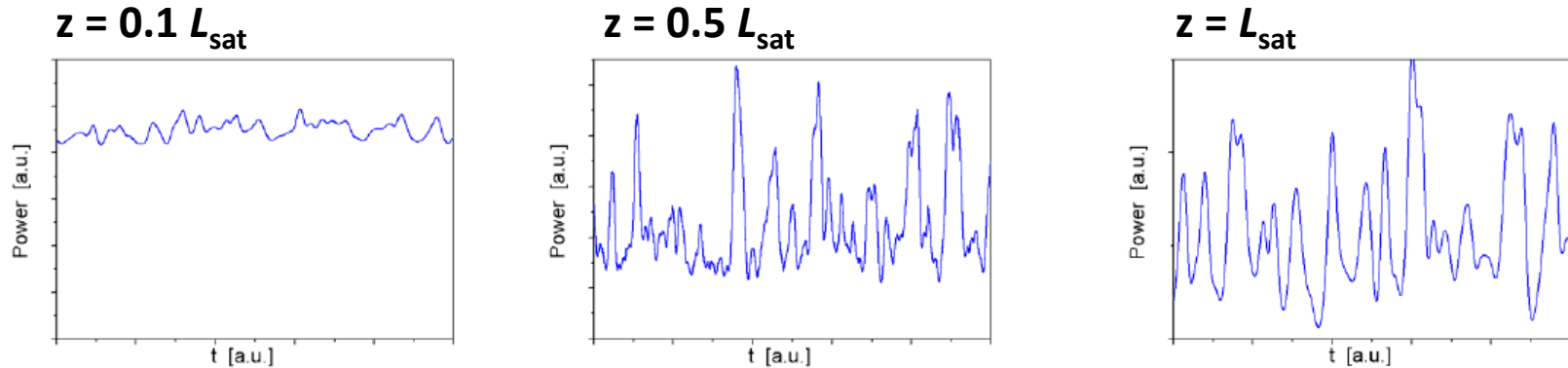
More SASE spikes are added beyond saturation.

- Radiation pulse consists of randomly distributed $N_u \lambda$ wave-packet
- Start-up noise is highest at high-peak-current parts of the bunch
- Microbunching is strong where radiation is most intense
- FEL gain is highest where electron microbunching is strong

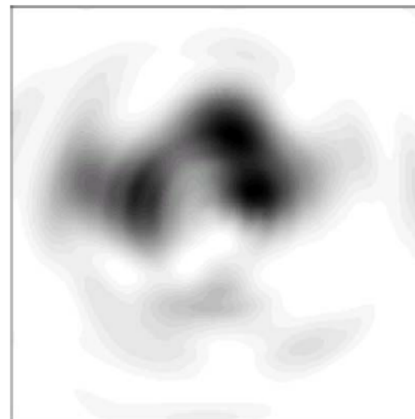
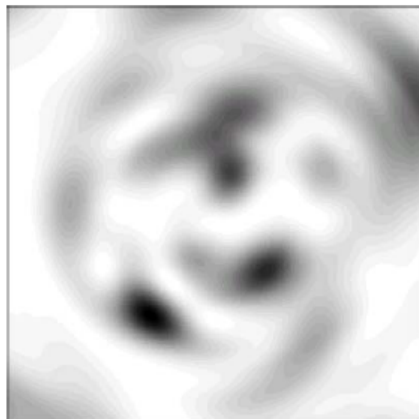
an instability



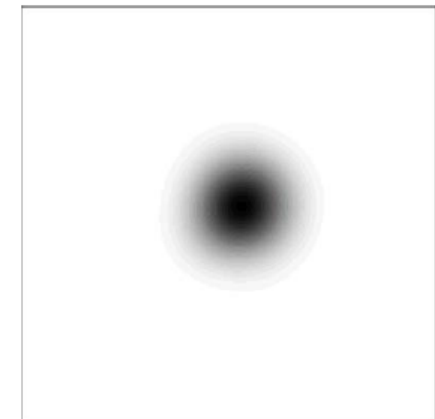
Temporal & Transverse Coherence



- Transverse (bottom) and longitudinal (top) distributions of the radiation intensity exhibit rather chaotic behaviour.

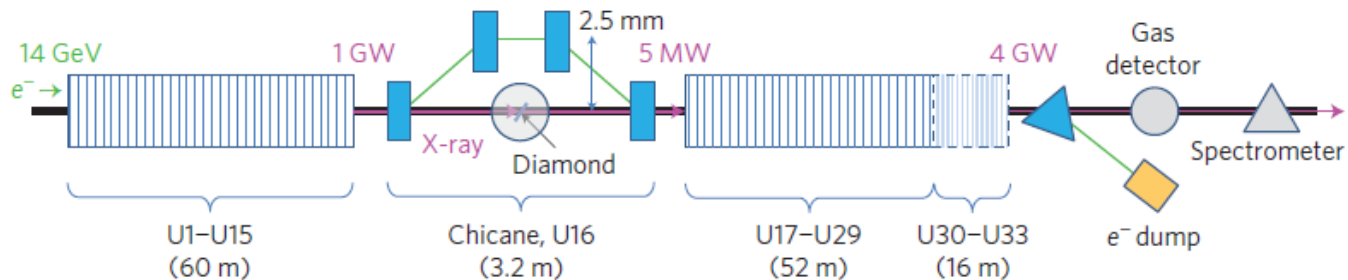


Full transverse coherence at saturation

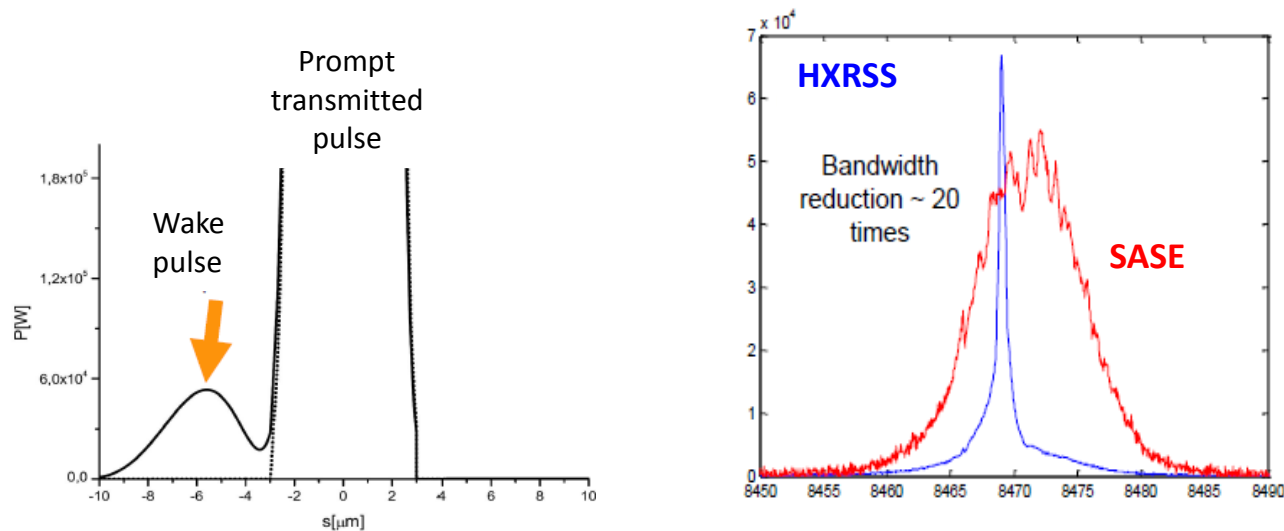


SASE Self-Seeding

Hard X-ray Self-Seeding (HXRSS) at Linac Coherent Light Source (SLAC)



The monochromatic wake pulse is used to seed the FEL interaction in subsequent undulators. The self-seeded FEL has a much narrower bandwidth (higher temporal coherence) than SASE.



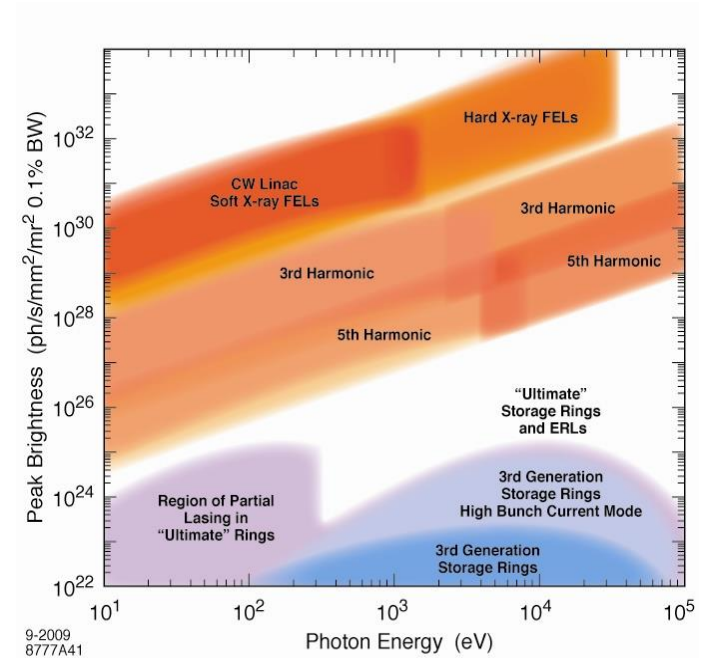
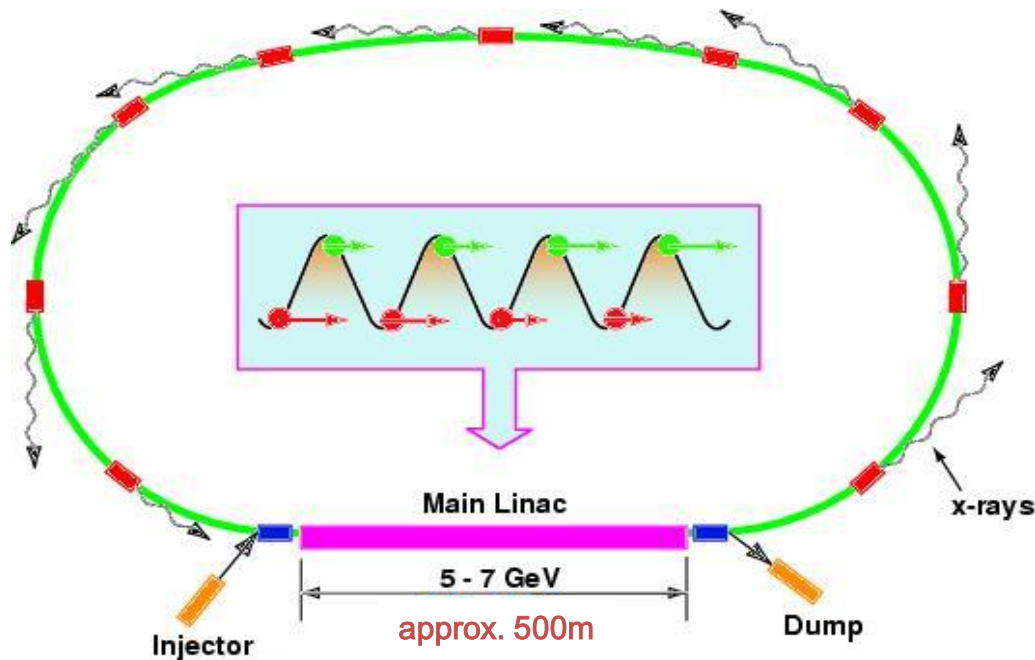
J. Amann et al., Nature Photonics, V. 6, Oct. 2012

Hard X-ray 4GLS Facilities

	LCLS-I	SACLA	EXFEL 2016	PAL HXFEL 2016	SwissFEL 2017	LCLS-II 2018
X-rays Pulse energy photons/pulse	12.8 keV 0.93 mJ 5E11	19.5 keV 0.16 mJ 7E10	24.7 keV 0.3 mJ 8E10	12.4 keV 0.3 mJ 1.5E11	12.4 keV 1.4 mJ 7E11	5 keV 25 μ J 3E10
Undulator period, K _{rms}	3.0 cm 2.5	1.8 cm 1.5	3.56 cm 2.3	2.44 cm 1.46	1.5 cm 1.1	3.2 cm 0.24
Electron beam energy	16.9 GeV	8 GeV	17.5 GeV	10 GeV	5.8 GeV	4 GeV
Linac type Linac length	NCRF S-band 1 km	NCRF C-band 0.4 km	SRF L-band 1.7 km	NCRF S-band 0.78 km	NCRF C- band 0.46 km	SRF L-band 0.4 km
Gun type Cathode	NCRF S-band Cu photo	Pulsed DC CeB ₆	NCRF L-band Cs ₂ Te photo	NCRF S-band Cu photo	NCRF S-band Cu photo	NCRF VHF Cs ₂ Te photo
RF macropulse Rep. rate	< 1 μ s 120 Hz	< 1 μ s 30 Hz	600 μ s 10 Hz	< 1 μ s 60 Hz	< 1 μ s 100 Hz	CW 930 kHz
# pulses/RF	1-2	1-2	2,700	1-2	1-2	N/A
Bunch charge	150 pC	200 pC	250 pC	200 pC	200 pC	20 pC
Bunch length	43 fs	<10 fs	50 fs	66 fs	42 fs	20 fs
Normalized emittance	0.4 μ m	0.6 μ m	0.6 μ m	<0.5 μ m	0.2 μ m	0.14 μ m

Energy Recovery Linac

Energy Recovery Linac (ERL)

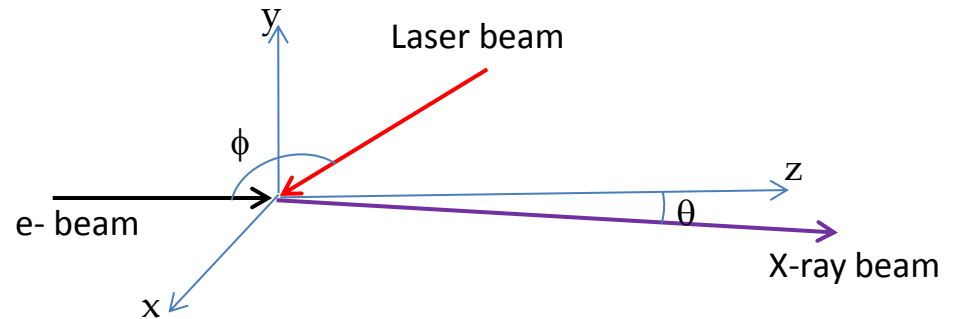


Each electron bunch is injected into the main linac and accelerated to GeV energies. Each electron bunch emits undulator radiation to provide X-rays to multiple users, and then returns to the same linac but at decelerating phase for energy recovery.

Inverse Compton Scattering

Inverse Compton Scattering wavelength

$$\lambda = \frac{\lambda_i}{2\gamma^2} \frac{1 + \gamma^2 \theta^2}{1 - \beta \cos \phi}$$



Special case, $\phi = 180^\circ$ (also called Compton backscattering)

The electrons in their rest frame see a laser wavelength with $1/2\gamma$ Doppler shift

Laser light is scattered in all directions in the electron rest frame

Boosted back to the lab frame, the scattered light has another $1/2\gamma$ Doppler shift

The final wavelength has $1/4\gamma^2$ Doppler shift ($4\gamma^2$ increase in frequency)

Compton backscattering wavelength

$$\lambda = \frac{\lambda_i}{4\gamma^2} (1 + \gamma^2 \theta^2)$$

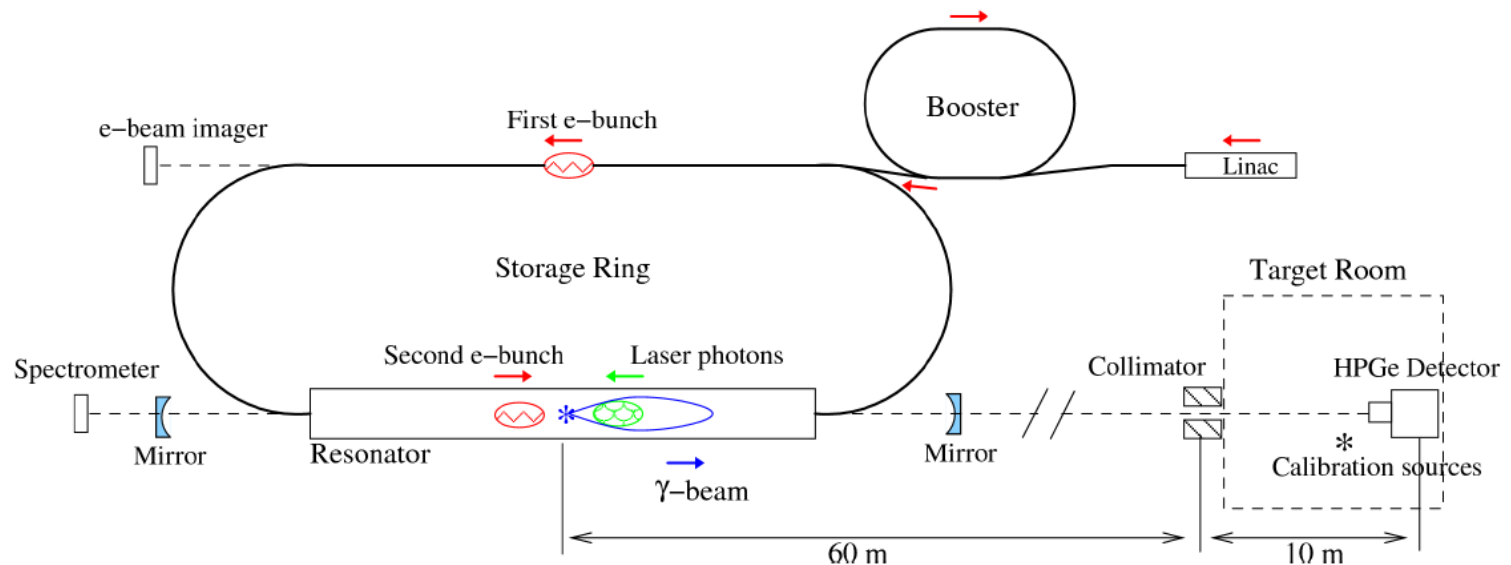
Inverse Compton Scattering properties

- Incoherent process
- Small scattering cross-section
- Wavelength- θ^2 correlation

FEL Intracavity Inverse Compton Scattering

The same electron bunches used to amplify the FEL radiation in an oscillator collide with the visible FEL photons that bounce back and forth between the resonator mirrors to generate high-energy ICS photons. Example:

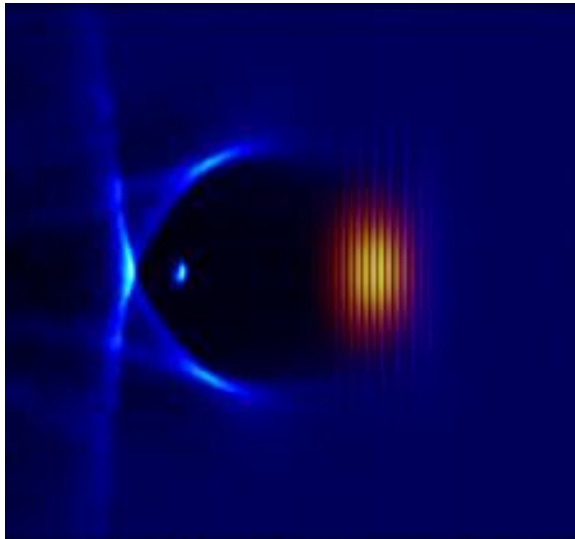
HIGS: High Intensity Gamma-ray Source



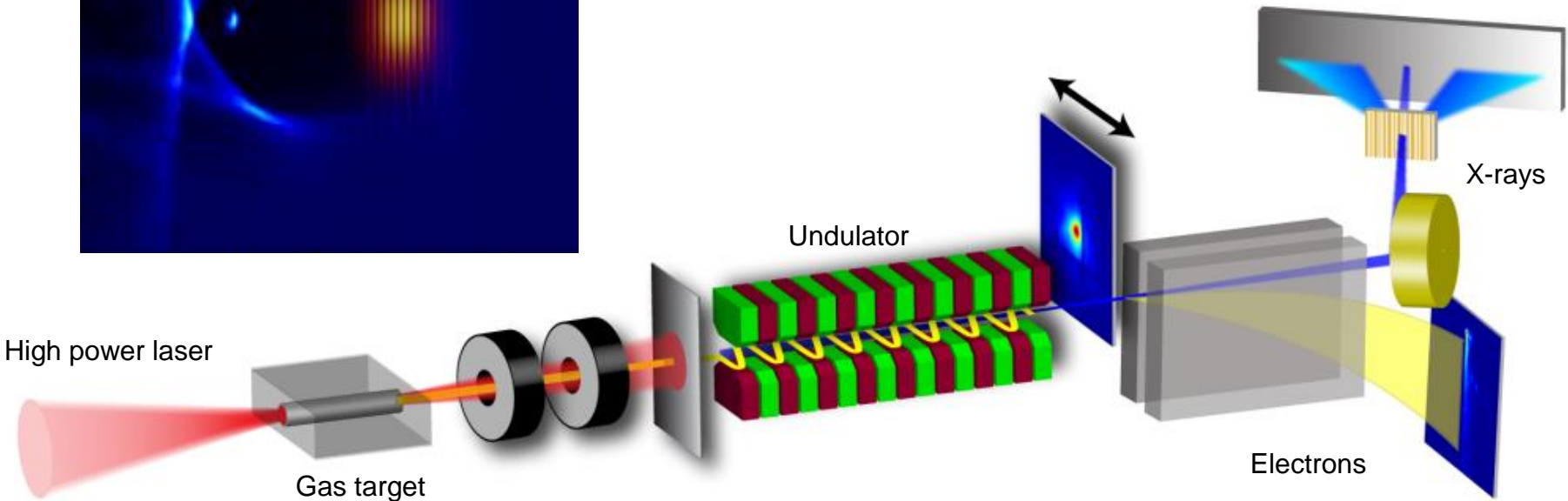
FEL Intracavity ICS produces high-energy γ photons with low-energy electron beams

C. Sun, "Characterizations of a Compton scattering gamma-ray beam" Duke University 2009

X-ray Sources driven by Laser Wakefield Accelerators



The intense laser pulse (orange) drives electrons out of the plasma creating a bubble, a void of electrons. The bright blue dot corresponds to trapped electrons that are accelerated by the wakefield in the bubble.



Laser wakefield accelerators can produce GeV, 10kA electron beams with $\sim 1 \mu\text{m}$ emittance but with large energy spread. LWA-generated electrons can be used to produce undulator radiation, and may be able to drive X-ray FELs in the future.

Summary

- Accelerator-based light sources cover the entire electromagnetic spectrum
- Synchrotron radiation (bending magnet, wiggler and undulator radiation) has unique properties that can be tailored to the users' needs
 - Bending magnet and wiggler radiation is broadband
 - Undulator radiation has narrow spectral lines
- X-ray FELs are the brightest coherent X-ray sources with
 - High photon flux
 - Femtosecond pulses
 - Full transverse coherence
 - Partial temporal coherence (SASE)
 - Narrow spectral lines with seeding techniques
- New developments in electron accelerators and radiation production can potentially lead to more compact sources of coherent X-rays.

References

- Synchrotron Radiation
 - “Synchrotron Radiation” by Helmut Wiedemann, Springer
 - “Soft X-rays and Extreme Ultraviolet Radiation” by David Attwood, Cambridge University Press
 - “An Introduction to Synchrotron Radiation: Techniques and Applications” by Philip Willmott, Wiley.
- Free-Electron Lasers
 - “Ultraviolet and Soft X-ray Free-Electron Lasers” by Peter Schmüser, Martin Dohlus and Jorg Rössbach, Springer Tract in Modern Physics
 - US Particle Accelerator School, “Physics of Free-Electron Lasers” by Dinh Nguyen and Quinn Marksteiner, 2014
<http://uspas.fnal.gov/materials/14UNM/UNM-FEL.shtml>
 - “Review of Free-Electron Laser Theory” by Zhirong Huang and Kwang-Je Kim, *Phys. Rev. Spec. Topics in Accel. Beams*, **10**, 034801 (2007).